Available online at www.sciencedirect.com

SCIENCE DIRECT®

Coordination Chemistry Reviews 241 (2003) 87–117

COORDINATION
CHEMISTRY REVIEWS

www.elsevier.com/locate/ccr

Silicon based phosphines with P–Si–P, P–C–Si–C–P and P–O–Si–O–P linkages and their coordination chemistry and catalytic applications☆

Maravanji S. Balakrishna *, P. Chandrasekaran, P.P. George

Department of Chemistry, Indian Institute of Technology Bombay, Mumbai 400 076, India

Received 9 August 2002; accepted 15 January 2003

Contents

Abbreviations: Acac, acetylacetonato group; o-An, o-$MeOC_6H_4$; Bihemp, (6,6′-dimethybiphenyl-2,2′-diyl)bis(diphenylphosphine); Binap, 2,2′-bis(diphenylphosphine)-1,1′-binaphthyl; BIPNOR, 2,2′,3,3′-tetraphenyl-4,4′,5,5′-tetramethyl-6,6′bis-phosphanorborna-2,5-dienyl; biPSiH, $MeHSi(CH_2CH_2CH_2PPh_2)_2$; biPSi, $R_2Si[(CH_2)_nPR_2]_2$; Bu, butyl; cht, cycloheptatriene; COD, cyclooctadiene; Cp, cyclopentadiene; Cp*, pentamethylcyclopentadiene; DCM, dichloromethane; DMP, dimethoxypropane; DME, dimethoxyethane; Dppm, bis(diphenylphosphino)methane; Dppe, bis(diphenylphosphino)ethane; ee, enantiomeric excess; Et, ethyl; *fac*, facial; M, metal; MCH, methylcyclohexane; Me, methyl; *mer*, meridional; Mes, mesityl; NBD, norbornadiene; NMR, nuclear magnetic resonance; Np, naphthalene; [O], oxidation; Ph, phenyl; Pr, propyl; R, alkyl/aryl group; r.t., room temperature; THF, tetrahydrofuran; TMNO, trimethylamine N-oxide; TMEDA, *N*,*N*,*N*′,*N*′-tetramethylethylenediamine; tmps, $MeSi(CH_2PMe_2)_3$; Si-triphos, $MeSi(CH_2PPh_2)_3$; trimpsi, $^{t}BuSi(CH_2PMe_2)_3$; triPSiH, $HSi(CH_2CH_2PPh_2)_3$.

☆ Through out the text all silicon-based ligands are referred in general as silylphosphines.

* Corresponding author. Fax: +91-22-2576-7152/2572-3480.

E-mail address: krishna@iitb.ac.in (M.S. Balakrishna).

doi:10.1016/S0010-8545(03)00018-3

Abstract

The synthesis and coordination chemistry of bis- and tris(phosphines) with P–Si–P, P–O–Si–O–P and P–C–Si–C–P linkages is reviewed. The catalytic reactions involving organometallic complexes of silylphosphines are presented. The silylbis- and tris(phosphines) show remarkable versatility in their coordination behavior with transition metals. The improved solubility of these ligands and their complexes facilitated spectroscopic studies to compliment the structural information obtained via single crystal X-ray diffraction studies. The syntheses and reactivity of other related acyclic and cyclic systems with P–N–Si–N–P and P-aryl–Si-aryl–P linkages are also briefly described.

Keywords: Silylalkylphosphines; Silylphosphinites; Coordination; Transition metal complexes; Bidentate; Catalysis

---

1. Introduction

The chemistry of compounds containing phosphorus and silicon has been considerably less explored when compared with those with phosphorus–carbon and phosphorus–nitrogen linkages in spite of the formal periodic relationship of silicon to carbon and the diagonal relationship between silicon and the nitrogen. The compounds containing direct phosphorus–silicon bonds or phosphorus–oxygen–silicon(esters) linkages form the important group of organic phosphorus compounds and are employed in a variety of industrial applications such as anti-foaming agents, polymeric materials, plasticizers, oil additives and flame-proofing agents. The silicon bound phosphorus(III) compounds or with phosphorus–oxygen–silicon(esters) and phosphorus–carbon–silicon linkages can act as ligands to stabilize transition metals in different oxidation states depending upon the nature of the substituents chosen on phosphorus centers. Platinum metal complexes of these compounds can be very good homogeneous catalysts for organic synthesis and also for co-polymerization.

To date, several bis-, tris- or polyphosphine systems have been developed having carbon [1–3] and nitrogen [4–7], as major spacers and to a little extent mixed ones, [8–11] whereas the compounds containing silicon atom as spacers are less extensive. This is because the phosphorus–silicon bonds are generally reactive and are susceptible to hydrolytic cleavage. In most cases, the compounds with these linkages can be used as precursor materials, which further react with appropriate reagents to give phosphorus–carbon or phosphorus–nitrogen bonds, by metathetical elimination of organosiliconhalides. However, mono-, bis- or polyphosphines with direct P–Si bonds or having P–O–Si and P–C–Si linkages have been utilized in transition metal chemistry and catalysis.

The present review is a survey of the coordination chemistry of bis-, tris or tetraphosphines with one of the spacers being a silicon atom. The coordination chemistry of a few silylmonophosphines is also described wherever they are appropriate but they are not discussed in detail; Okazaki and coworkers have very recently reviewed the synthesis and reactivity of silylmonophosphine complexes [12]. Attention is also given to the catalytic application of these complexes. Fryzuk and coworkers have extensively studied the chemistry of a novel nitrogen bridged heterofunctional bis(phosphine) system containing two organosilicon spacers. Verkade has also developed a novel triazasilatrane derivative and its coordination chemistry. Although, these systems are not included in this review, brief outline is given in Section 4 while discussing the other related ligand systems.

2. Synthesis of ligands

The various synthetic routes and the reaction conditions for the preparation of a variety of silylphosphines are given in Tables 1–4. The reactions of potassium diphenylphosphide with silylhalides afford bis- or tris(phosphines) in moderate yields (Eq. (1)). The syntheses of silylphosphines with carbon spacers involve the reaction of alkyl or aryl substituted silanes containing alkene groups with appropriate secondary phosphines under photochemical conditions as shown in Eq. (2). The reaction of appropriate lithium alkylphosphines with silylhalides also gives the silylalkylphosphines (Eq. (3)). The Grignard reagents of alkylsilanes react with halophosphines to give the corresponding silylalkylphosphines (Eq. (4)).

$$R_nSiCl_{4-n} + (4-n)KPPh_2 \rightarrow R_nSi(PPh_2)_{4-n} \quad (n = 1 \text{ or } 2) \tag{1}$$

$$R_nSi(CH{=}CH_2)_{4-n} + (4-n)HPR'_2 \xrightarrow{h\nu} R_nSi(CH_2CH_2PR'_2)_{4-n} \quad (n = 1 \text{ or } 2) \tag{2}$$

$$R_nSiCl_{4-n} + (4-n)LiCH_2PR'_2 \rightarrow R_nSi(CH_2PR'_2)_{4-n} \quad (n = 1 \text{ or } 2) \tag{3}$$

$$R^1R^2Si(CH_2MgX)_2 + XPR_2 \rightarrow R^1R^2Si(CH_2PR_2)_2 \tag{4}$$

$$R^1R^2SiCl_2 + R_2P(O)H \xrightarrow{Et_3N} R^1R^2Si(OPR_2)_2 \tag{5}$$

Silyldiphosphites of the type $[(R^1O)_2PO]_2SiR^2R^3$ can be conveniently prepared in high yield by the reaction of the secondary phosphites with $Cl_2SiR^2R^3$ in the presence of NEt_3 (Eq. (5)) [13,14]. Similarly, silyltris(phosphites) can be prepared as shown in Eq. (6). This route can also

Table 1
Experimental details for the synthesis of silylbis(phosphine) ligands

Reactants (amount in molar ratio)	Reaction conditions (°C) or UV/solvent/time (h)	Product (yield, %)	Reference
$HMeSi(CH{=}CH_2)_2$ (1) + PPh_2H (3)	$h\nu$/THF, Et_2O/60	$MeHSi((CH_2)_2PPh_2)_2$ (60)	[20]
$HPhSi(CH{=}CH_2)_2$ (1) + PPh_2H (3)	$h\nu$/THF, Et_2O/60	$PhHSi((CH_2)_2PPh_2)_2$ (98)	[20]
$HPhSi(CH{=}CH_2)_2$ (1) + PPh_2H (1) + PCy_2H (1)	$h\nu$/THF, Et_2O/50	$PhHSi[(CH_2)_2PCy_2][(CH_2)_2PPh_2]$ (94)	[20]
$HMeSi(CH{=}CH_2)_2$ (1) + PCy_2H (1)	$h\nu$/THF, Et_2O/50	$MeHSi[(CH_2)_2PCy_2]_2$	[20]
$HPhSi(CH{=}CH_2)_2$ (1) + PCy_2H (2.1)	$h\nu$/Et_2O/50	$PhHSi[(CH_2)_2PCy_2]_2$ (93)	[20]
$HMeSi(CH_2CH{=}CH_2)_2$ (1) + PPh_2H (2)	$h\nu$/Et_2O/150	$MeHSi[(CH_2)_3PPh_2]_2$ (97)	[20]
$HPhSi(CH_2CH{=}CH_2)_2$ (1) + PPh_2H (2)	$h\nu$/Et_2O/150	$PhHSi[(CH_2)_3PPh_2]_2$	[20]
$HMeSi[(CH_2)_2CH{=}CH_2)]_2$ (2) + PPh_2H (1)	$h\nu$/Et_2O/114	$MeHSi[(CH_2)_4PPh_2]_2$ (88)	[20]
$Me_2Si(CH_2MgCl)_2$ (1) + PPh_2Cl (2)	0/Et_2O/12	$Me_2Si(CH_2PPh_2)_2$	[21]
$Me_2Si(CH_2PPh_2)_2$ (1) + O_2	25/CH_2Cl_2/4	$Me_2Si(CH_2P(O)Ph_2)_2$	[21]
$Me_2Si(CH_2PPh_2)_2$ (4) + S (1)	40/CH_2Cl_2/2	$Me_2Si(CH_2P(S)Ph_2)_2$ (74)	[21]
$Me_2Si(CH_2PPh_2)_2$ (1) + KseCN (1)	25/CH_3CN/1	$Me_2Si(CH_2P(Se)Ph_2)_2$ (67)	[21]
Me_2SiCl_2 (1) + $LiCH_2PMe_2$ (2)	25/THF/–	$Me_2Si(CH_2PMe_2)_2$	[21]
Me_2SiCl_2 (1) + $KPPh_2$ (2)	25/C_6H_6/12	$Me_2Si(PPh_2)_2$	[22]
$(ClMe_2Si)_2(SiMe_2)$ (1) + $KPPh_2$ (2)	25/C_6H_6/12	$(Ph_2PMe_2Si)_2(SiMe_2)$ (65)	[22]
$(ClMe_2Si)_2$ (1) + $KPPh_2$ (2)	25/C_6H_6/12	$(Ph_2PMe_2Si)_2$ (80)	[22]
$Me_2Si(CH{=}CH_2)_2$ (1) + $HPPh_2$ (2)	$h\nu$/Et_2O/150	$Me_2Si[(CH_2)_2PPh_2]_2$	[23]
$PPh(Np)(Me)(BH_3)$ + Me_2SiCl_2 + *sec*-BuLi	−78/THF/3	$Me_2Si[(CH_2P(Ph)(Np)BH_3]_2$	[23]
$Me_2Si[(CH_2P(Ph)(Np)BH_3]_2$	25/morpholine/12	$Me_2Si[(CH_2P(Ph)(Np)]_2$	[23]
$(C_5H_4N)NH(PPh_2)$ (2) + LDA + Cl_2SiMe_2 (1)	−50/toluene/4	$Me_2Si[N(C_5H_4N)PPh_2]_2$	[24]
$Me_2Si[N(C_5H_4N)PPh_2]_2$ (1) + Se (2)	80/toluene/1	$Me_2Si[N(C_5H_4N)P(Se)Ph_2]_2$	[24]
$ZrCp_2(H)Cl$ (1) + $SiHMe(CH_2CH{=}CH_2)_2$ (1) + PPh_2Cl (2)	25/C_6H_6/16	$MeHSi[(CH_2)_3PPh_2]_2$ (51)	[25]
$ZrCp_2(H)Cl$ (1) + $SiH(CH_2CH{=}CH_2)_3$ (1) + PPh_2Cl (2)	25/C_6H_6/18	$HSi(^nPr)[(CH_2)_3PPh_2]_2$	[25]
$ZrCp_2(H)Cl$ (1) + $SiH_2(CH_2CH{=}CH_2)_2$ (1) + PPh_2Cl (2)	25/C_6H_6/16	$H_2Si[(CH_2)_3PPh_2]_2$ (59)	[25]
$ZrCp_2(H)Cl$ (1) + $SiHMe(CH_2CH{=}CH_2)_2$ (1) + $P(n\text{-hex})_2Cl$ (2)	25/C_6H_6/16	$MeHSi[(CH_2)_3P(n\text{-hex})_2]_2$ (46)	[25]
$ZrCp_2(H)Cl$ (1) + $SiHMe(CH_2CH{=}CH_2)_2$ (1) + PPhBzCl (2)	25/C_6H_6/16	$MeHSi[(CH_2)_3PPhBz]_2$ (56)	[25]
I_2SiH_2 (1) + $LiP(SiMe_3)_2$ (2)	−30/DME/–	$H_2Si[P(SiMe_3)_2]_2$ (68)	[26]
$H_2ISiSiIH_2$ (1) + $LiP(SiMe_3)_2$ (2)	−75/pentane/–	$[(Me_3Si)_2PSiH_2]_2$ (3)	[26]

afford the analogous germanium and tin compounds. The relative rates of formation of products are sensitive to the nature of the substituents on both phosphorus and silicon and follow the order: [SiMeH] > [$SiMe_2$] > [$SiMe(CH{=}CH_2)$] > [SiMePh] > [$SiPh_2$]. ^{31}P-NMR investigations have suggested that the nature of the silicon substituents has only a small effect on through-bond electronic induction or hybridization at the phosphorus atoms of the free bis(phosphites). Complexation of these bis(phosphites) to transition metals stabilizes the ligand towards hydrolysis compared with the uncoordinated ligands, which are otherwise highly air and moisture sensitive [15]. Experimental details are given in Table 4.

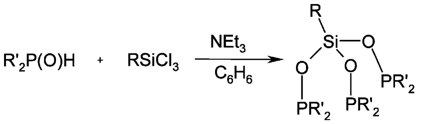

(6)

Although several phosphinoalkylsilanes are known, corresponding phosphinoarylsilanes are less extensive.

Table 2
Experimental details for the synthesis of silyltriphosphines

Reactants (amount in molar ratio)	Reaction condition (°C) temperature or UV/solvent/time (h)	Product (yield (%))	Reference
$PhSi(CH{=}CH_2)_3$ (1) + PPh_2H (3.1)	$h\nu$/THF, Et_2O/0	$PhSi[(CH_2)_2PPh_2]_3$	[20]
$HSi(CH{=}CH_2)_3$ (1) + PCy_2H (3)	$h\nu$/THF, Et_2O/70	$HSi[(CH_2)_2PCy_2]_3$	[20]
$HSi(CH_2CH{=}CH_2)_3$ (1) + PPh_2H (3)	$h\nu$/neat/150	$HSi[(CH_2)_3PPh_2]_3$(trimPSiH)	[20]
$MeSi(CH{=}CH_2)_3$ (1) + PPh_2H (3)	$h\nu$/neat/72	$MeSi[(CH_2)_2PPh_2)]_3$	[82]
Bu_2PLi (3) + $MeSiCl_3$ (1)	−80/Et_2O/–	$MeSi(PBu_2)_3$	[76]
$MeSi(SiMe_2Cl)_3$ (1) + $KPPh_2$ (3)	25/C_6H_6/–	$MeSi(SiMe_2PPh_2)_3$ (50)	[22]
$HSi(CH_2CH{=}CH_2)_3$ (1) + $HPPh_2$(3) + $ZrCp_2HCl$	25/C_6H_6/18	$HSi[(CH_2)_3PPh_2]_3$	[25]
$MeSiCl_3$ (1) + $LiCH_2PMe_2$ (3)	−78/Et_2O/2.5	$MeSi(CH_2PMe_2)_3$(tmps)	[69]

Table 3
Synthesis of silylbis(phosphinites)

Reactants (amount in molar ratio) [a]	Reaction condition (°C)/solvent/time (h)	Product (Yield (%))	Reference
$\mathrm{Ph_2P(O)H}$ (2)+$\mathrm{Me_2SiCl_2}$ (1)	25/$\mathrm{C_6H_6}$/24	$\mathrm{(Ph_2PO)_2SiMe_2}$ (70)	[13]
$\mathrm{(MeO)_2P(O)H}$ (2)+$\mathrm{Me_2SiCl_2}$ (1)	25/toluene/48	$\mathrm{[(MeO)_2PO]_2SiMe_2}$ (96)	[15]
$\mathrm{(MeO)_2P(O)H}$ (2)+$\mathrm{Ph_2SiCl_2}$ (1)	25/toluene/96	$\mathrm{[(MeO)_2PO]_2SiPh_2}$ (81)	[15]
$\mathrm{(MeO)_2P(O)H}$ (2)+$\mathrm{MePhSiCl_2}$ (1)	25/toluene/48	$\mathrm{[(MeO)_2PO]_2SiMePh}$ (99)	[15]
$\mathrm{(MeO)_2P(O)H}$(2)+$\mathrm{Me(CH{=}CH_2)SiCl_2}$ (1)	25/toluene/48	$\mathrm{[(MeO)_2PO]_2SiMe(CH{=}CH_2)}$ (87)	[15]
$\mathrm{(MeO)_2P(O)H}$ (2)+$\mathrm{MeHSiCl_2}$ (1)	25/toluene/20	$\mathrm{[(MeO)_2PO]_2SiMeH}$ (91)	[15]
$\mathrm{(EtO)_2P(O)H}$ (2)+$\mathrm{Me_2SiCl_2}$ (1)	25/toluene/48	$\mathrm{[(EtO)_2PO]_2SiMe_2}$ (78)	[15]
$\mathrm{(EtO)_2P(O)H}$ (2)+$\mathrm{Ph_2SiCl_2}$ (1)	25/toluene/96	$\mathrm{[(EtO)_2PO]_2SiPh_2}$ (87)	[15]
$\mathrm{(EtO)_2P(O)H}$ (2)+$\mathrm{MePhSiCl_2}$ (1)	25/toluene/96	$\mathrm{[(EtO)_2PO]_2SiPhMe}$ (82)	[15]
$\mathrm{(PhO)_2P(O)H}$ (2)+$\mathrm{Me(CH{=}CH_2)SiCl_2}$ (1)	25/toluene/48	$\mathrm{[(EtO)_2PO]_2SiMe(CH{=}CH_2)}$ (85)	[15]
$\mathrm{(EtO)_2P(O)H}$ (2)+$\mathrm{MeHSiCl_2}$ (1)	25/toluene/20	$\mathrm{[(EtO)_2PO]_2SiHMe}$ (85)	[15]
$\mathrm{Me_2SiCl_2}$ (1)+$\mathrm{(tol)_2P(O)H}$ (2)	25/toluene/16	$\mathrm{[(tol)_2PO]_2SiMe_2}$	[29]
$^n\mathrm{Bu_2P(O)H}$ (2)+$\mathrm{Me_2SiCl_2}$ (1)	25/$\mathrm{C_6H_6}$/48	$(^n\mathrm{Bu_2PO)_2SiMe_2}$ (78)	[27]
$\mathrm{(PhO)_2P(O)H}$ (2)+$^t\mathrm{Bu_2SiCl_2}$ (1)	25/$\mathrm{C_6H_6}$/48	$\mathrm{(Ph_2PO)_2Si}\,^t\mathrm{Bu_2}$	[28]

[a] 2 equiv. of $\mathrm{Et_3N}$ was used to abstract HCl in all reactions.

Table 4
Synthesis of silyltris(phosphinites)

Reactants (amount in molar ratio) [a]	Reaction condition (°C)/solvent/time (h)	Product (yield (%))	Reference
$\mathrm{Ph_2P(O)H}$ (3)+$\mathrm{MeSiCl_3}$ (1)	25/$\mathrm{C_6H_6}$/48	$\mathrm{(Ph_2PO)_3SiMe}$	[13]
$^n\mathrm{Bu_2P(O)H}$ (3)+$\mathrm{MeSiCl_3}$ (1)	25/$\mathrm{C_6H_6}$/48	$(^n\mathrm{Bu_2PO)_3SiMe}$ (73)	[13]
$\mathrm{(MeO)_2P(O)H}$ (3)+$\mathrm{MeSiCl_3}$ (1)	25/pentane/72	$\mathrm{[(MeO)_2PO]_3SiMe}$ (85)	[30]
$\mathrm{(EtO)_2P(O)H}$ (3)+$\mathrm{MeSiCl_3}$ (1)	25/pentane/72	$\mathrm{[(EtO)_2PO]_3SiMe}$ (90)	[30]
$\mathrm{(MeO)_2P(O)H}$ (3)+$\mathrm{PhSiCl_3}$ (1)	25/pentane/72	$\mathrm{[(MeO)_2PO]_3SiPh}$ (99)	[30]
$\mathrm{(EtO)_2P(O)H}$ (3)+$\mathrm{PhSiCl_3}$ (1)	25/pentane/72	$\mathrm{[(EtO)_2PO]_3SiPh}$ (99)	[30]
$\mathrm{(MeO)_2P(O)H}$ (3)+$\mathrm{(CH_2{=}CH)SiCl_3}$ (1)	25/pentane/72	$\mathrm{[(MeO)_2PO]_3Si(CH{=}CH_2)}$ (82)	[30]
$\mathrm{(EtO)_2P(O)H}$ (3)+$\mathrm{(CH_2{=}CH)SiCl_3}$ (1)	25/pentane/72	$\mathrm{[(EtO)_2PO]_3Si(CH{=}CH_2)}$ (91)	[30]

[a] 3 equiv. of $\mathrm{Et_3N}$ was used to abstract HCl in all reactions.

Attempts to synthesize silyarylphosphine derivative using the reaction of the Grignard reagent, $\mathrm{Me_2(H)SiC_6H_4MgBr}$-*o* with $\mathrm{PPh_2Cl}$ via exchange metalation led to the isolation of an inseparable mixture of compounds $\mathrm{Me_2HSiC_6H_4(CH_2PPh_2)}$-*o* and $\mathrm{Me_2HSiCH_2C_6H_4(PPh_2)}$-*o*. In contrast, lithiation of *o*-tolyldiphenylphosphine in the presence of TMEDA or (*o*-bromobenzyl)diphenylphosphine, followed by quenching with chlorodimethylsilane afforded the compounds above in their pure form without contamination by one another. In the latter reaction, addition of either dichloromethylsilane or trichlorosilane instead of chlorodimethylsilane affords analogues of biPSiH (**I**) and triPSiH (**II**), respectively, as shown in Scheme 1 [16].

The reaction of diphenylether with ^{n}BuLi in THF followed by the addition of dimethydichlorosilane affords 10,10-dimethylphenoxasilin in 45% yields. Further treatment of this compound with *sec*-BuLi/TMEDA and then with $\mathrm{PPh_2Cl}$ gives crystalline sixanthphos (**III**) in 68% yield (Scheme 2). This ligand is used in rhodium-catalyzed hydroformylation reactions in which the aromatic groups induce very high regioselectivity; the details are discussed in Section 5 [17].

Treatment of $\mathrm{R_3Si(CH{=}CH_2)}$ with $\mathrm{Cp_2Zr(H)Cl}$ followed by reaction with $\mathrm{PPh_2Cl}$ provides a high-yield

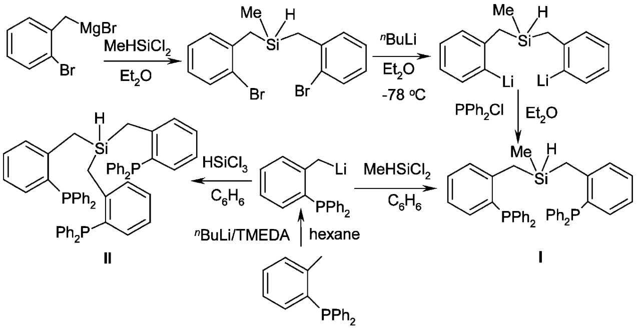

Scheme 1.

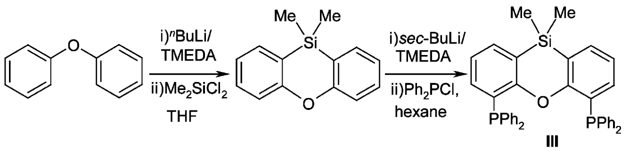

Scheme 2.

route to $Ph_2PCH_2CH_2SiR_3$ through the hydrozirconated intermediate $Cp_2Zr(CH_2CH_2SiR_3)Cl$. Similarly, the diallyl ($R_2Si(CH{=}CH_2)_2$ or $RHSi(CH{=}CH_2)_2$) or triallyl silanes ($RSi(CH{=}CH_2)_3$ or $HSi(CH{=}CH_2)_3$) afford corresponding bis- and tris(phosphine) derivatives, respectively (see Table 1). The stereoselective synthesis of several cyclic derivatives containing P, Si, Ge or Sn were effected using zirconium diene complexes as described in Schemes 3 and 4 [18,19].

The range and generality of other synthetic methods for the preparation of silylphosphines and silylphosphinites are illustrated in Tables 1–4.

3. Coordination chemistry of silylphosphines

The coordination chemistry of silylphosphines is less extensive when compared with the carbon or nitrogen bridged ligand system. Although, the first silicon-bridged bis(phosphine) was prepared as early as 1970, [32] the coordination chemistry was not explored.

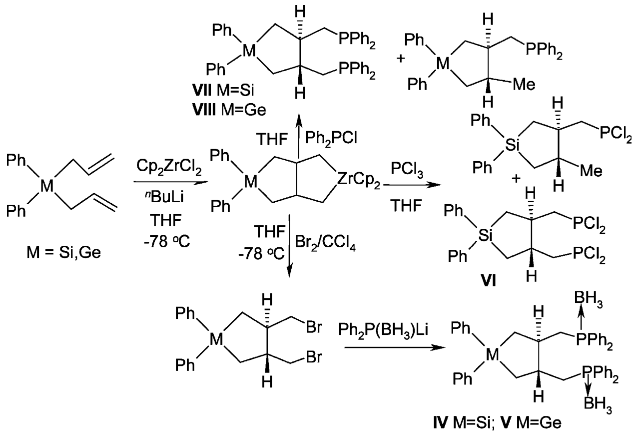

Scheme 3.

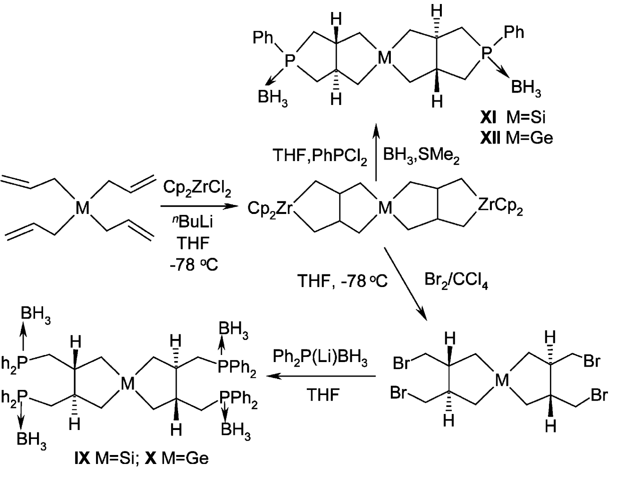

Scheme 4.

The silylphosphines show remarkable versatility in their coordination behavior. They can readily act as monodentate, bridged or chelate bidentate ligands with most of the transition metals. The metal complexes containing one or more monodentate silylphosphines can be used as synthons in designing novel binuclear and trinuclear complexes. Further, silylphosphines containing cyclopentadienyl group, are used in the synthesis of metallocene derivatives. Interestingly, silylphosphines with one or two Si–H bonds may eliminate hydrogen in the form of H_2 or HX (X = alkyl or halide) with appropriate metal reagents under appropriate reaction conditions to establish a M–Si σ-bond anchored by two or three phosphorus donor centers.

The review will be a survey of silylphosphines of the type $R_{4-n}Si(Q{-}PR'_2)_n$ ($n = 2, 3$; Q = C, O or none), i.e. with direct P–Si bonds or having P–O–Si and P–C–Si linkages and their transition metal chemistry with the different elements along the periodic table with special emphasis on the reactivity of the complexes and their catalytic applications.

3.1. Group 1

The first lithium monophosphinomethanide complex containing a trimethylsilyl group was obtained from the reaction of ^{n}BuLi and $HC(SiMe_3)_2(PMe_2)$ in a mixture of hexane and THF. The compound **1** is a dinuclear, six-membered ring in a chair conformation with lithium atoms having coordination number 3 [33]. The structure was confirmed by single crystal X-ray analysis. The reaction of bis(diphenylphosphino)-trimethylsilylmethane with ^{n}BuLi in the presence of TMEDA leads to the formation of lithium adducts **2** and **3** [34]. These adducts are similar to phosphinomethanide analogues. The monophosphine, $Me_2PCH_2SiMe_3$ reacts with ^{t}BuLi in the presence of TMEDA to give a cage complex **4** with twist conformation as shown in Scheme 5 [35]. The reaction of dimethylchlorosilylphosphine, $ClSi(Me_2)$-CH_2PPh_2 with LiC_5H_5 followed by the addition of ^{n}BuLi affords compounds **6** and **7** which are further used to make metallocene derivatives; details are included in Group 4 discussion [33].

Reaction of lithium shot with chlorobis{bis(trimethylsilyl)methyl}phosphine, $PClR_2$ ($R = CH(SiMe_3)_2$) in THF resulted in the formation of a first isolated uncomplexed phosphidolithium, $[Li(\mu\text{-}PR_2)_2]_2$ (**8**). Also, this is the first among crystalline $[LiX]_n$ compounds to have the $[Li(\mu\text{-}X)]_2$ structure [36]. The synthesis and reactivity of this compound is shown in Scheme 6. The lithium phosphide behaves either as a PR_2 source (transfer agent) or a Lewis acid.

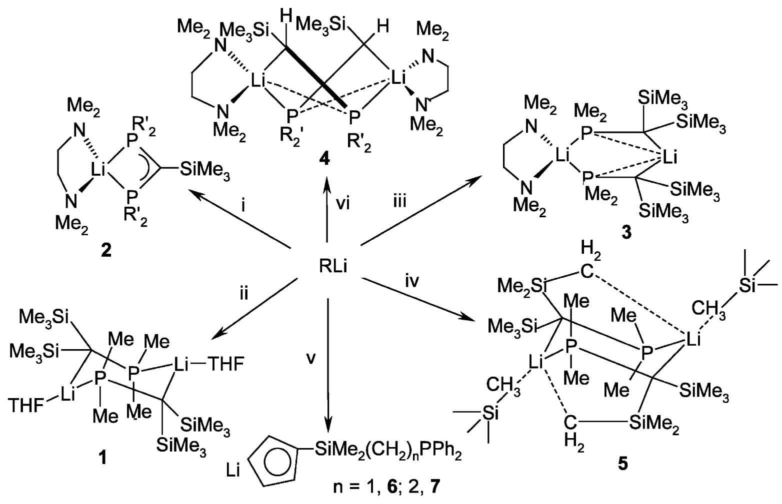

i) R = ^{n}Bu, R' = Me or Ph, $Me_3SiCH(PR'_2)_2$, TMEDA / hexane, -78 °C
ii) R = ^{t}Bu, $HC(PMe_2)(SiMe_3)_2$,(1:2) hexane /THF
iii) R=^{n}Bu· $HC(PMe_2)(SiMe_3)_2$, hexane, -78 °C; iv) R = ^{t}Bu, $HC(PMe_2)(SiMe_3)_2$,(1:2) $SiMe_4$
v) $C_5H_5Si(CH_3)_2(CH_2)_nPPh_2$, hexane, R = ^{n}Bu, 27 °C; vi) ^{t}BuLi, TMEDA, THF

Scheme 5.

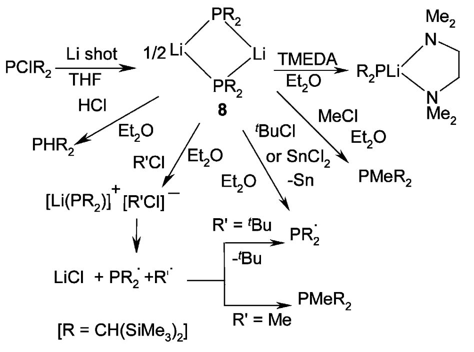

Scheme 6.

3.2. Group 2 and Group 3

Although, there are reports about phosphines with strong Lewis basicity forming adducts with Group 2 and 3 metals [4], to the best of our knowledge there are no reports on the interaction of silylphosphines with Group 2 elements. However, Glindelberger and Arnold have reported the reaction of homoleptic magnesium selenolate, $Mg[SeSi(SiMe_3)_2]$ with trimPSi to form $Mg[SeSi(SiMe_3)_3](trimPSi)$ (**9**) as colorless crystalline solid (See Scheme 7). The structure was determined by single crystal X-ray diffraction. The metal is bound to two selenolates and two PMe_2 groups of trimPSi. The Mg–P bond distances are consistent with the predicted covalent value (2.65 Å) [37]. There is no report of interaction of silylphosphines with Group 3 and also Group 13 elements. In a few cases while synthesizing the silylphosphines, BH_3 adducts were formed in order to protect the lone pairs on the phosphorus(III) reagents, (see Schemes 3, 4, 46 and 7).

3.3. Group 4

A wide variety of complexes of silylphosphines have been prepared with Group 4 metal derivatives. The reaction of Cp^*TiCl_3 with an excess of $LiBH_4$ in diethyl ether followed by the addition of 1 equiv. of ^{n}BuLi in the presence of $^t BuSi(CH_2PMe_2)_3$, (trimPSi) affords the dark brown complex **10** in 55% yield [38]. The ligand is bidentate. The X-ray crystal structure of the complex **10** confirms the presence of a bidentate BH_4^- unit. The reductive carbonylation of tripod phosphine complex, $[^t BuSi(CH_2PPh_2)_3TiCl_3(THF)]$ using sodium naphthalenide in THF under CO atmosphere gives the titanium(0) complex, $[^t BuSi(CH_2PPh_2)_3Ti(CO)_4]$ (**11**) [39]. In the absence of CO, the reduction leads to the formation of a deep red–purple solution, from which the arene complex **12** was formed in 40% yield as shown in Scheme 8 [40]. Treatment of **12** with CO rapidly yields the same titanium(0) complex **11**.

Schore has reported [41] the preparation of zirconocene dihalide and the ferrocene derivatives of lithium salts **6** and **7** and their utilization as metallo ligands to

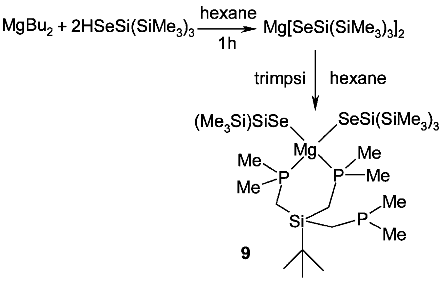

Scheme 7.

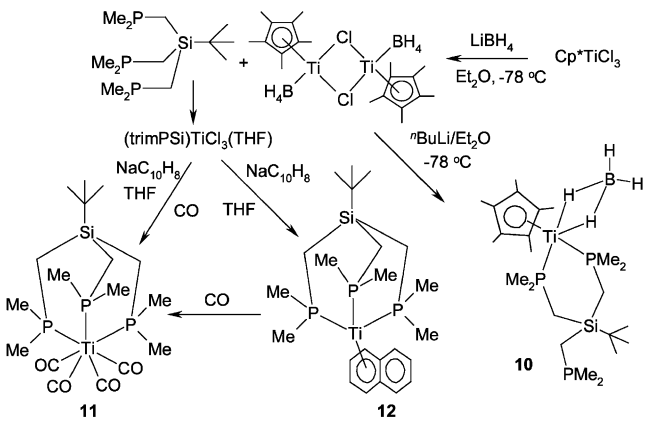

Scheme 8.

generate heterobimetallics with appropriate transition metal derivatives. The reaction of $LiC_5H_4Si(Me_2)(CH_2)_nPPh_2$ ($n = 1$, 2) with $ZrCl_4$ affords $[Cl_2Zr\{C_5H_4Si(Me_2)(CH_2)_nPPh_2\}_2]$ (**13**, **14**) [41,42] as shown in Scheme 9. The analogous ferrocene derivatives were also prepared by treating $LiC_5H_5Si(Me_2)CH_2PPh_2$ with $FeCl_2$ in diethylether at room temperature (r.t.) (Scheme 24). The conversion of dichloro derivative **14** into both its monohydride **15** and dihydride **16** derivatives was achieved using $LiAlH(^tOBu)_3$ and $LiAlH_4$ as reducing agents, respectively. The monohydride reacts with simple alkenes to give the alkyl derivative **17** similar to other chlorozirconocene hydride systems [43]. The reaction of **14** with $Co_2(CO)_8$ leads to the isolation of oligomeric product **18**.

3.4. Group 5

Girolami and Gardner have reported the synthesis and crystal structure of a vanadium(I)tricarbonylhydride complex, $[\{^tBuSi(CH_2PPh_2)_3\}V(CO)_3H]$ (**20**) obtained by reducing $[\{^tBuSi(CH_2PPh_2)_3\}VCl_3(THF)]$ (**19**) with sodium naphthalenide in THF under CO atmosphere as shown in Scheme 10 [39].

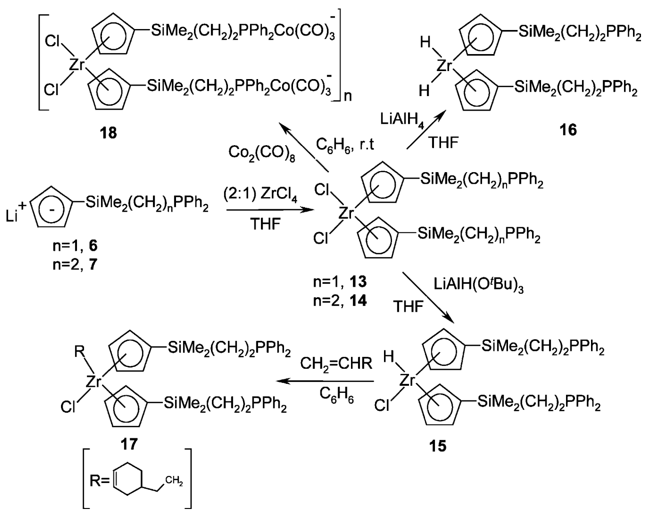

Scheme 9.

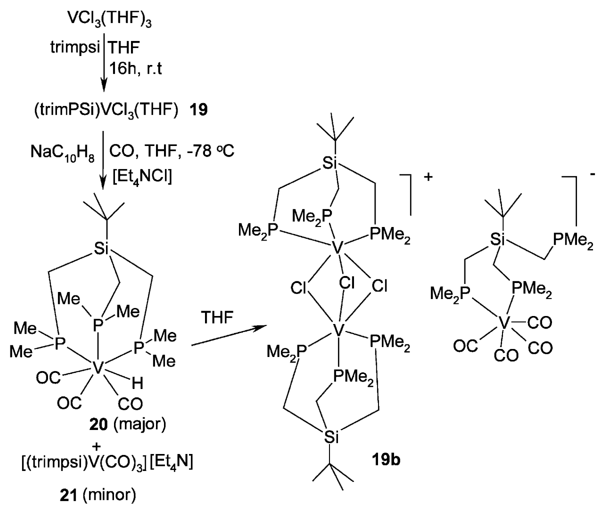

Scheme 10.

Treatment of the hexacarbonyl metallates $[Et_4N][M(CO)_6]$ (M = Nb Ta) in DME with iodine followed by the addition of $^tBuSi(CH_2PMe_2)_3$ afforded the new tricarbonyl iodide complexes $[(trimPSi)M(CO)_3I]$ (M = Nb, **22**; M = Ta, **23**) in high yield as air-stable microcrystalline solids with trimPSi acting as a tridentate ligand. Reduction of **22** and **23** generated air-sensitive yellow solutions of tricarbonyl derivatives which on treatment with diazald (*N*-methyl-*N*-nitroso-*p*-toluenesulfonamide) at −78 °C afforded the first nitrosyl complexes of niobium and tantalum, $[M(\eta^3\text{-trimPSi})(CO)_2NO]$ (M = Nb, **24**; Ta, **25**) (Scheme 11). The thermally stable crystalline complexes **24** and **25** were characterized by X-ray studies [44]. The geometries at the metal centers are essentially octahedral and in both structures the ligand exhibits a trigonal-twist distortion about the Si–M vector similar to the crystallographi-

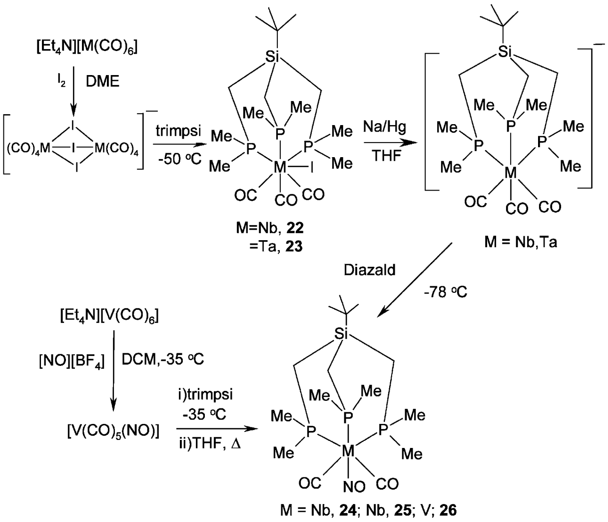

Scheme 11.

cally characterized titanium (**11**, **12**) and vanadium (**20**) complexes of the same ligand [39,40].

Treatment of trimpsi with vanadium analogue, $[Et_4N][V(CO)_6]$ did not give the expected $[(trimpsi)V(CO)_3I]$, instead, the known hydride complex **20** was obtained in low yield. However, vanadium analogue, $[(\eta^2\text{-trimpsi})V(CO)_3NO]$ was obtained as an oil when trimpsi was reacted with 1 equiv. of $V(CO)_5(NO)$ in dichloromethane. The IR spectrum supports the structural formulation of $[(\eta^2\text{-trimpsi})V(CO)_3NO]$ by showing $\nu(CO)$ bands at 1990, 1904 and 1813 cm^{-1} and $\nu(NO)$ at 1560 cm^{-1}. On refluxing the $[(\eta^2\text{-trimpsi})V(CO)_3NO]$ in THF for 1 h results in the disappearance of the original $\nu(CO)$ and $\nu(NO)$ bands and the appearance of new $\nu(CO)$ bands at 1919 and 1833 cm^{-1} and a new $\nu(NO)$ band at 1600 cm^{-1} suggesting loss of a CO group and formation of a dicarbonyl complex $[(\eta^3\text{-trimpsi})V(CO)_2NO]$ (**26**) in moderate yield. The $^{31}P\{^1H\}$-NMR spectrum of **26** consists of two octets at 5 ppm (2P) and −10 ppm (1P), respectively, for phosphorus atoms *trans* to CO and NO, respectively, with $^1J_{PV}$ couplings of 2204 and 130 Hz. The X-ray structure confirms octahedral geometry around the vanadium center. The reaction of $(trimpsi)VCl_3(THF)$ (**19**) with 4 equiv. of sodium naphthalenide in THF in the presence of excess of CO followed by the addition of $[Et_4N][Cl]$ afforded cationic complex $[(trimpsi)V(CO)_3][Et_4N]$ (**21**) as yellow powder in 5% yield along with slightly impure hydride complex, $(trimpsi)V(CO)_3H$ (**20**). Crystallization of hydride complex in THF resulted in the formation of a few green crystals, the X-ray analysis revealed them to be $[(trimpsi)V(\mu\text{-}Cl)_3V(trimpsi)]^+[(\eta^2\text{-trimpsi})V(CO)_4]^- \cdot 3THF$ (**19b**) as shown in Scheme 10. The cation consists of two face-sharing octahedral bridged by three chlorides and capped by two trimpsi ligands. The anion is an $18e^-$ octahedral species with one of the arms of trimpsi is pendant. The anion which is isoelectronic with $[V(CO)_6]^-$ represents first structurally characterized phosphine-substituted derivative of $[V(CO)_6]^-$ [45].

The 17-electron bis-arene derivative of niobium, $[Nb(\eta^6\text{-toluene})_2]$ reacts with tmps to give zero-valent half sandwich complex **27**. The complex **27** on treatment with potassium followed by hydrolysis of resulting anion gives a green niobium hydride complex **28** as shown in Scheme 12 [46,47]. The X-ray structure of **27** reveals the symmetrical bonding of the toluene ring with metal to ring distances of 1.827 (2) Å.

3.5. Group 6

The reaction of bis(2-diphenylphosphinobenzyl)dichlorosilane with 1 equiv. of $Na_2[Cr(CO)_5]$ in THF affords the pincer type complex **29** in 34% yield. Photolysis of **29** results in the 1,2 shift of the phosphorus centers through stepwise carbonyl elimination to give the tricarbonyl complex **31** involving a tetracarbonyl intermediate **30** as shown in Scheme 13 [48].

The reaction of trimPSi adduct, $[^tBuSi(CH_2PMe_2)_3]CrCl_3$ with alkyl-lithium reagents afforded the first octahedral chromium(III) trialkyl complexes, $[^tBuSi(CH_2PMe_2)_3]CrR_3$ (R = Me, **32**; R = ^{n}Bu, **33**) stabilized by a tridentate phosphine ligand (Scheme 14). Both the complexes are characterized by single crystal X-ray analysis. Interestingly, the *n*-butyl derivative is found to be remarkably resistant to β-elimination [49].

The reaction of silylbis(phosphine), $Me_2Si(CH_2PPh_2)_2$ with $Mo(CO)_6$ and $[Mo(CO)_4Br_2]$ at r.t. afford chelate complexes **34** and **35** as shown in Scheme 15 [50]. Similarly, the reaction of silyldiphosphites with $[M(CO)_4NBD]$ afford *cis*-tetracarbonyl derivatives **36**–**42** as shown in Eqs. (7) and (8) [28]. The structures of complexes **40** and **41** were confirmed by X-ray diffraction studies. Both **40** and **41** consist of slightly distorted octahedral monomers in which the diphosphite ligands

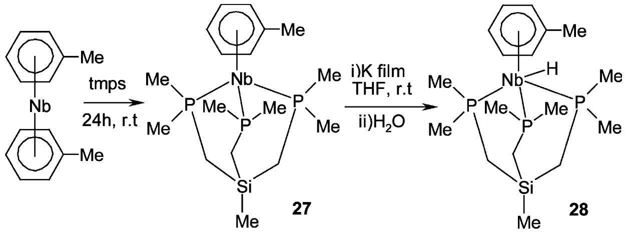

Scheme 12.

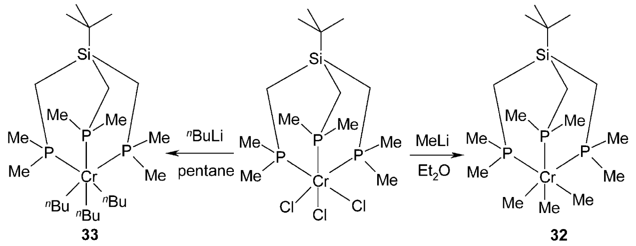

Scheme 14.

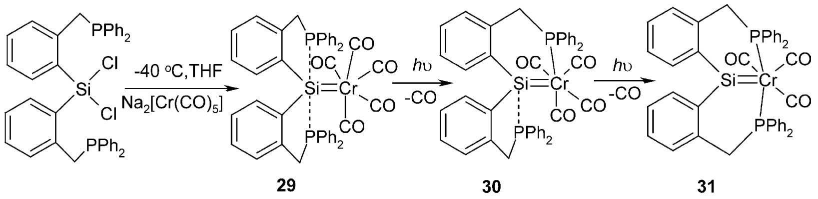

Scheme 13.

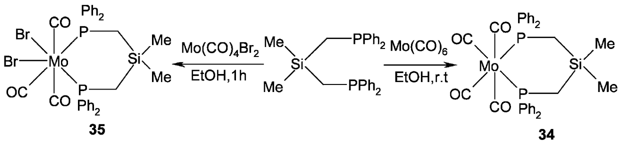

Scheme 15.

occupy mutually *cis*-positions [51]. The structures of **36** and **37** are also confirmed by X-ray studies [28].

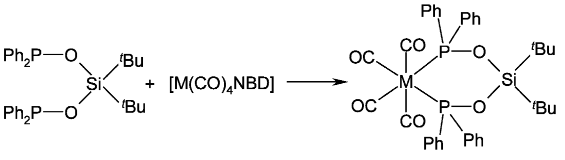

M=Cr, **36**; Mo, **37**; W, **38**

(7)

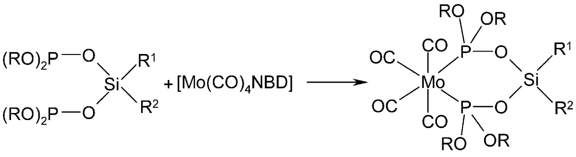

39, R=R^1=R^2=Me
40, R=Me, R^1=R^2= Ph
41, R=R^1=Me, R^2= Ph
42, R=R^1=Me, R^2= CH=CH$_2$

(8)

A few silyldiphosphine ligands were generated at the metal centers starting from versatile complex *cis*-[Mo(CO)$_4$(PPh$_2$Cl)$_2$] in which the two phosphorus centers can undergo nucleophilic substitutions. *Cis*-[Mo(CO)$_4$(PPh$_2$Cl)$_2$] readily reacts with a variety of nucleophiles, HX in the presence of Et$_3$N to yield complexes, *cis*-[Mo(CO)$_4$(PPh$_2$X)$_2$] (**43**–**52**) as shown in Scheme 16. Gray and coworkers have reported extensive NMR correlation studies on this type of complex [52–54]. The structures of **48**, **49** and **50** were determined by X-ray diffraction studies. The coordination geometry of the molybdenum in each of these complexes is a slightly distorted octahedron consisting of four carbonyl groups and two phosphorus centers *cis* to each other. The Mo–P distances are shorter in **48** and **49** (2.428 and 2.425 Å) than in **50** (2.488 Å). This is expected since the phosphites are poorer σ-donors and better π-acceptors than phosphines, the greater π-acceptor ability of the phosphites results in a greater multiple bonding between Mo and P and shorten bond lengths [55]. The reaction of *cis*-[Mo(CO)$_4$(PPh$_2$NH$_2$)$_2$] first with ^{n}BuLi and then with Cl$_2$SiR$_2$ yields unique metallacycles, *cis*-[Mo(CO)$_4$(PPh$_2$NH)$_2$SiR$_2$] (**53**, **54**) as shown in Scheme 17 [56].

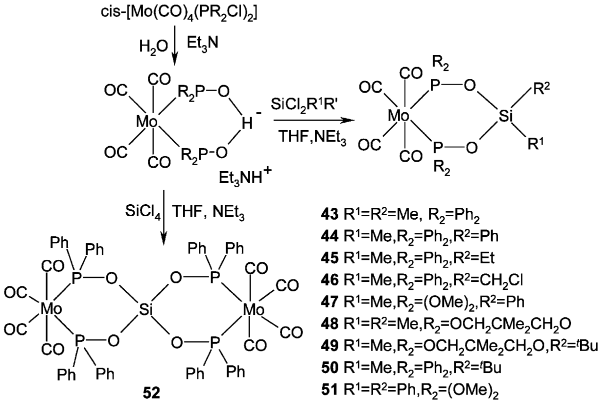

43 R^1=R^2=Me, R$_2$=Ph$_2$
44 R^1=Me,R$_2$=Ph$_2$,R^2=Ph
45 R^1=Me,R$_2$=Ph$_2$,R^2=Et
46 R^1=Me,R$_2$=Ph$_2$,R^2=CH$_2$Cl
47 R^1=Me,R$_2$=(OMe)$_2$,R^2=Ph
48 R^1=R^2=Me,R$_2$=OCH$_2$CMe$_2$CH$_2$O
49 R^1=Me,R$_2$=OCH$_2$CMe$_2$CH$_2$O,R^2=^{t}Bu
50 R^1=Me,R$_2$=Ph$_2$,R^2=^{t}Bu
51 R^1=R^2=Ph,R$_2$=(OMe)$_2$

Scheme 16.

The silylated triphosphites of the type, {(R′O)$_2$PO}$_3$SiR″ (R′ = Me or Et; R″ = Me, Ph or CH=CH$_2$) readily react with [Mo(CO)$_4$NBD] and [Mo(CO)$_3$(η^6-C$_7$H$_8$)] to afford [Mo(CO)$_4${η^2-{(MeO)$_2$PO}$_3$SiMe}] (**55**) and *fac*-[Mo(CO)$_3${η^3-{(R′O)$_2$PO}$_3$SiR″}] (**56**–**58**), respectively, as shown in Scheme 18. The structure of **56** has been determined by X-ray diffraction studies [30]. The structure consists of distorted-octahedral molecules in which the triphosphite acts as a tridentate ligand through all three of the phosphorus atoms. The chelate rings adopt a twist-boat conformation that may be partly due to the flexibility of the phosphite ligands.

The phosphorus–silicon heterocycle nonaphenylcyclotrisilaphosphane, [R$_2$Si–PR]$_3$ reacts with [Mo(CO)$_3$(cht)] to give *fac*-[Mo(CO)$_3${η^3-[R$_2$Si–PR]$_3$}] (**59**) which is the first example of this class of compound (Eq. (9)) [57]. The complex shows two sharp ν(CO) bands at 1931 and 1838 cm^{-1} and three ν(SiP) bands at 393, 333 and 305 cm^{-1} corresponding to the structural formulation.

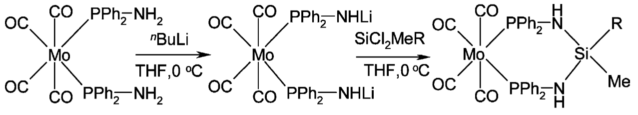

53 R = Me
54 R = Ph

Scheme 17.

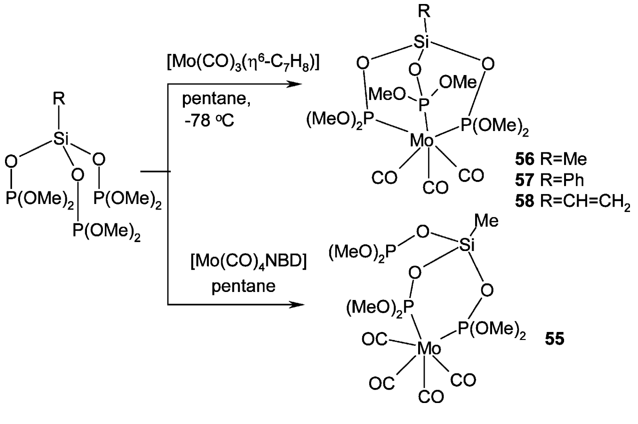

Scheme 18.

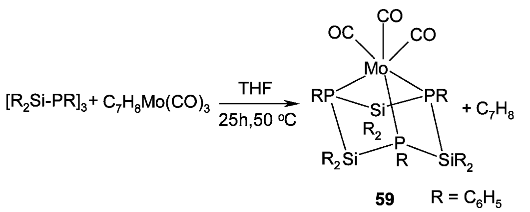

(9)

The sealed tube reaction of [W(η^6-C_6H_5Me)$_2$] with 2 equiv. of $MeSi(CH_2PPh_2)_3$ heated at 200 °C for 2 days led to the isolation of half-sandwich complex [W(η^6-C_6H_5Me){$MeSi(CH_2PPh_2)_3$}] (**60**) as shown in Scheme 19. Treatment of **60** with NH_4BF_4 in THF gives the hydride cationic complex **61** in 70% yield [58].

3.6. Group 7

The silylbis(phosphine), $Me_2Si(CH_2PPh_2)_2$ reacts with $MnBr(CO)_5$ to give the chelate complex **62** [50]. Activation of a C–H bond in a CH_3–Si group by manganese has been reported by Ressner et al. [59] in the thermal reaction between $MeMn(CO)_5$ and $Me_2Si(CH_2PPh_2)_2$ which leads to the formation of complex **63** as shown in Scheme 20. The ligand $Me_2Si(CH_2PPh_2)_2$ behaves as a typical chelating tridentate ligand with manganese in a typical octahedral environment. The methyl group on manganese abstracts one hydrogen atom from one of the silylmethyl group to establish a methylene bridge between the metal and silicon center followed by the elimination of 1 mol of methane.

The reactions of silylbis(phosphites) with $MnBr(CO)_5$ afford tricarbonyl complexes [$MnBr(CO)_3${$P(OMe)_2$-O}$_2SiR^2R^3$] (**64**–**67**) in good yield. The *facial* geometry of the manganese complexes is supported by the three v(CO) bands in the IR spectrum. Further, the structure of one of the complexes (**64**) is confirmed by a single-crystal X-ray diffraction study [14,15]. Similarly the silylbis(phosphinite), $Me_2Si[OP(tol)_2]_2$ reacts smoothly with $MnBr(CO)_5$ at r.t. in toluene to afford the tricarbonyl derivative **68** in good yield [29].

3.7. Group 8

Silyltris(phosphine), $MeSi(CH_2PMe_2)_3$(tmps) readily reacts with [Fe(η^6-C_6H_6)(PMe_3)$_2$] to give diamagnetic [Fe(η^4-C_6H_6)(η^3-tmps)] (**69**) in high yield. The η^4-coordination mode of the benzene was confirmed by low temperature NMR spectroscopic studies. The complex **69** readily undergoes displacement of the coordinated benzene with CO (1 atm) to give [Fe(η^3-tmps)(CO)$_2$] (**70**) in quantitative yield. Treatment of **69** with diphenylacetylene gives green crystals of 18-electron complex, [(η^3-tmps)Fe(η^2-PhC≡CPh)] (**71**) in 60% yield. The ^{13}C-NMR spectrum of **71** shows the chemical shift of acetylenic carbon atoms at 187 ppm expected for coordinated alkyne ligands as four-electron donors. When **69** is heated to 50 °C with ethylene, the bridging μ-vinylidene–μ-dihydrido complex (**75**) is formed as shown in Scheme 21. The structure of **75** is confirmed by a single crystal X-ray diffraction study. The molecule contains two tmp ligands bound to iron centers and bridged by one vinylidene and two hydrido ligands. The geometry around the iron atoms is octahedral and they share a face. Although, the iron–iron bond is short at 2.428(1) Å, electron-counting considerations suggest that there is no need to extrapolate a direct Fe–Fe bond [60]. The complex **75** can also be prepared by reducing [{(η^3-tmps)Fe}$_2$(μ-Cl)$_3$]Cl (**81**) with sodium amalgam in toluene under ethylene (2 atm) as shown in Scheme 22. The complex **81** was prepared in quantitative yield by reacting $FeCl_2 \cdot 2THF$ with tmps in a mixture of toluene–dichloromethane (1:3). Although, the complex was formulated as a monomeric species [Fe(η^3-tmps)Cl_2] (**80**) in the earlier communication, [61] the authors have reformulated it as a dimer after studying its reactivity [60] and comparing it with analogous complex of etriphos, [{$MeC(CH_2PEt_2)_3$}-Fe(μ-Cl)$_3$Fe{$MeC(CH_2PEt_2)_3$}]BPh_4 (**82**) whose crystal

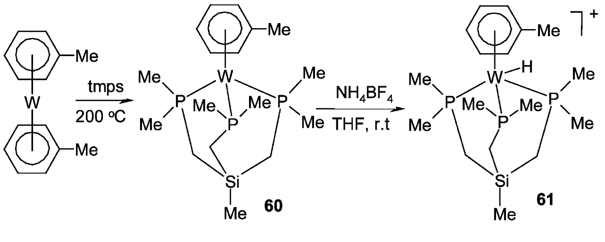

Scheme 19.

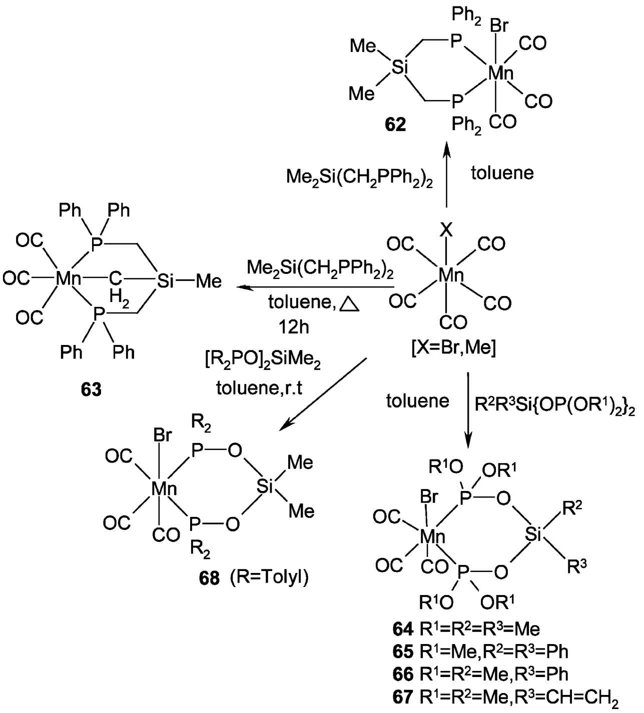

Scheme 20.

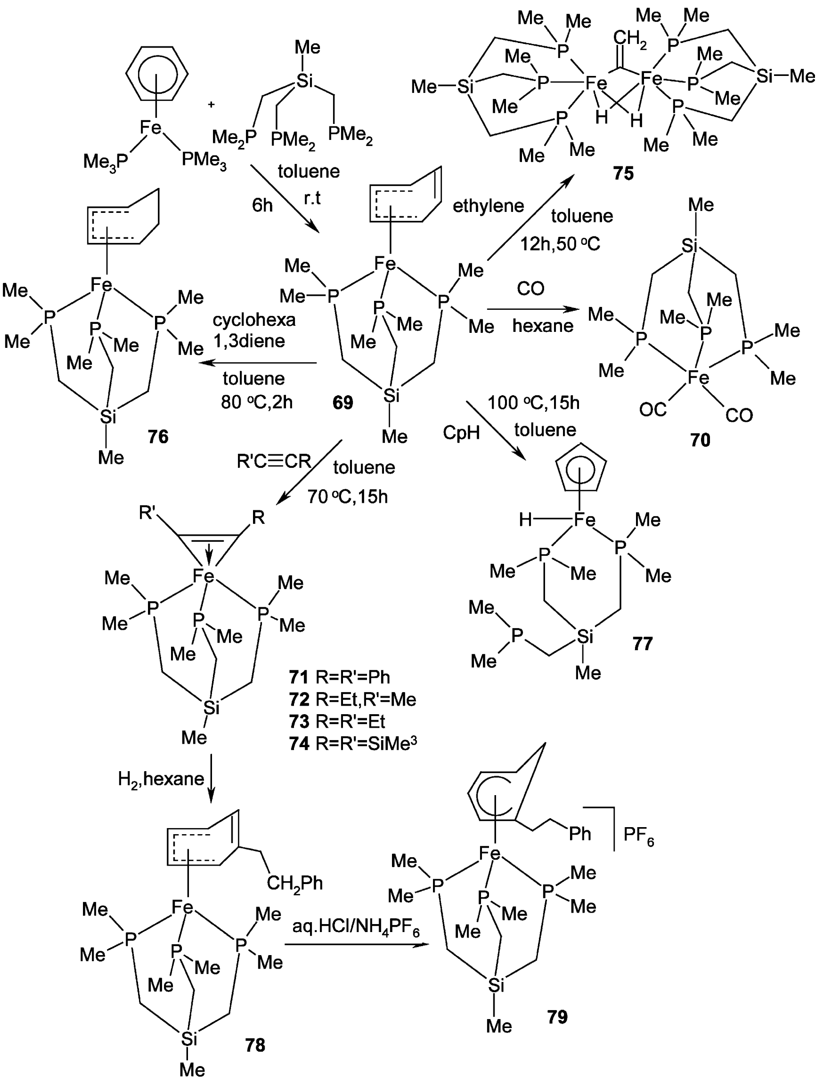

Scheme 21.

structure has been determined [62]. The dimer **81** reacts readily with $[Mg(C_4H_6)(THF)_2]$ to give the η^4-butadiene complex $[\{\mu\text{-tmps}\}Fe(\eta^4\text{-}C_4H_6)]$ (**83**) as pentane soluble yellow crystals. Treatment of **81** with an excess of sodium cyclopentadienide in THF, followed by addition of NH_4PF_6, gives the complex **84** in good yield. The details are summarized in Scheme 22.

The reaction of $[Fe(\eta^6\text{-}C_6H_6)(PMe_3)_2]$ with tmps results in phosphine substitution and arene ring slippage to form $[Fe(\eta^4\text{-}C_6H_6)(tmps)]$ (**69**). In contrast, the reaction of $[Fe(\eta^6\text{-}C_6H_6)dmpe]$ with tmps at 60 °C gave the arene-displacement product, [Fe(dmpe)(tmps)] (**85**) which on further treatment with NH_4PF_6 affords a pseudo-octahedral protonated product **86** as an orange crystalline solid (Scheme 23) [63].

The direct reaction of silylphosphine, $LiC_5H_5\text{-}Si(Me_2)(CH_2)_nPPh_2$ with anhydrous $FeCl_2$ in diethylether affords ferrocene derivatives **87** and **88** as red–orange oils which very slowly solidify at r.t. under nitrogen. The ferrocene derivatives react with nickel halides under a variety of conditions to produce the corresponding nickel(II) halide complexes **89**–**92** as shown in Scheme 24 [64].

The reaction of **88** with nickel chloride in 1:1 ratio yields the mono nickel complex **91** whereas the same reaction with nickel bromide gives a mixture of monomeric (**92**) and dimeric (**94**) complexes which coexist both in the solid state and in solution. Reaction of **87** with the molybdenum complex, $[Mo(CO)_4(NBD)]$ in refluxing methylcyclohexane gives a mixture of *cis*,*cis* (**96**) and *trans*,*trans* (**97**) and *cis*,*trans* (**98**) dimeric species as indicated by IR and NMR spectroscopic data. The reaction of **87** with $[BrMn(CO)_5]$ in benzene solution also yields a mixture of isomers (**99** and **100**) as indicated by NMR and IR spectroscopic data [65].

The ferrocene derivative **87** reacts readily with $Co_2(CO)_8$ in benzene at r.t. to give complex **101** with the Co–Co fragment intact. The complex **101** is found

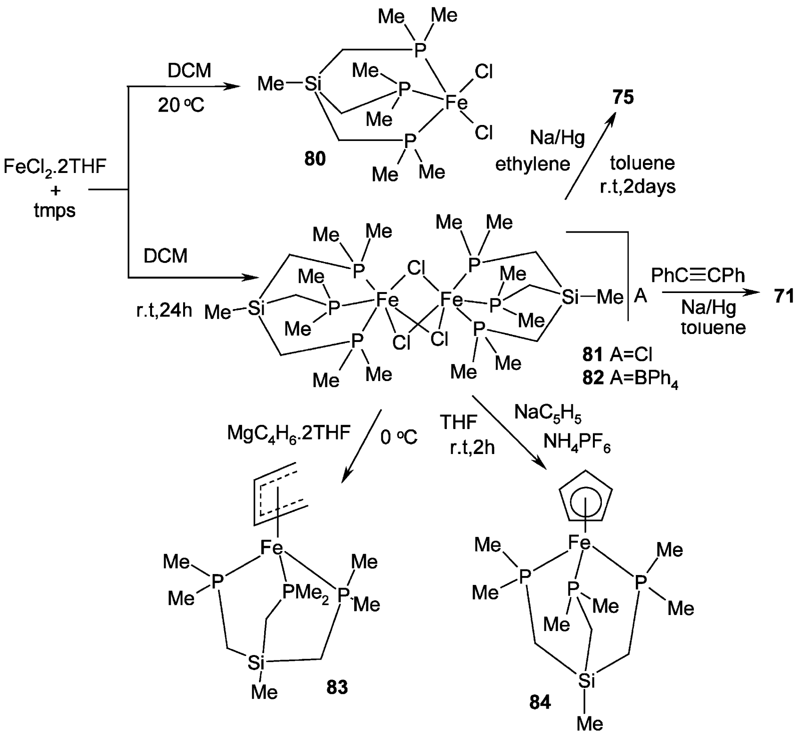

Scheme 22.

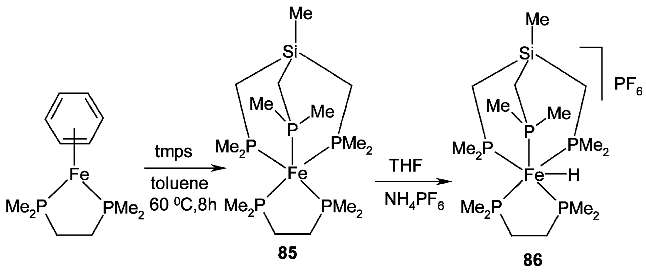

Scheme 23.

to be very sensitive to oxygen in solution. Bubbling of air through a chloroform solution of **101** leads to the formation of phosphine oxide derivative **102** with the elimination of cobalt moieties. Reduction of **101** using sodium amalgam gives product **103** whose spectroscopic data suggest the presence of $NaCo(CO)_4$. An alternative and cleaner method for reduction of metal–metal bond is the addition of KH in THF solution followed by bis(triphenylphosphine)iminium chloride which precipitates KCl and produces the salt **103** as shown in Scheme 25. These transformations clearly demonstrate the effective chemical independence of the two metal sites. Both oxidation and reduction occur at the cobalt center without any chemical modifications at the ferrocene site. Thus the individuality is effectively preserved in these silylphosphine bound binuclear systems [65].

The silyltriphosphine, $MeSi(CH_2PMe_2)_3$ (tmps) reacts with $[(Me_3P)_4RuCl_2]$ in toluene to give the octahedral

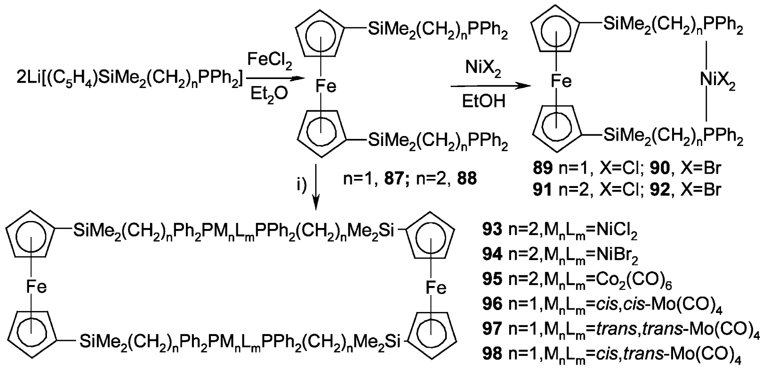

i) NiX_2 (X=Cl or Br) or $Co_2(CO)_8$ or $[Mo(CO)_4NBD]$

Scheme 24.

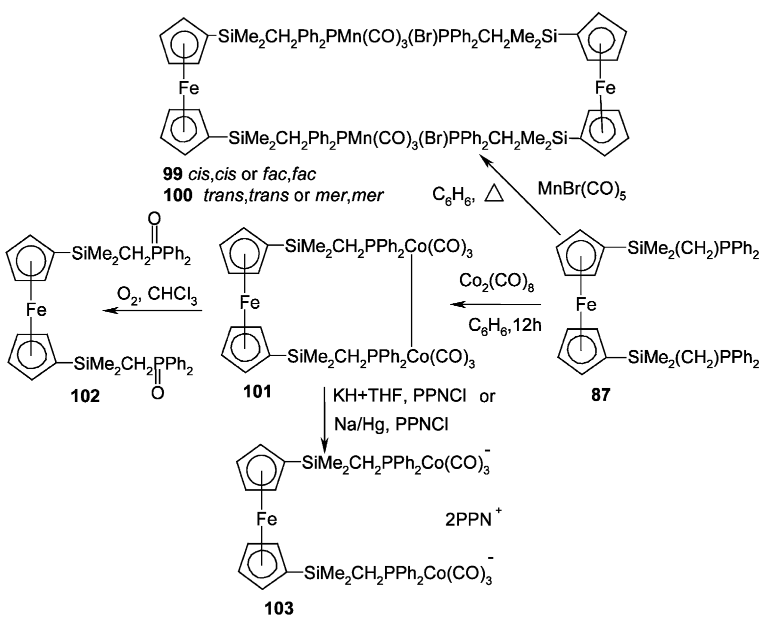

Scheme 25.

complex, [$RuCl_2(tmps)(PMe_3)$] (**104**) in 88% yield. The reduction of **104** with Na/Hg in benzene affords hydrido derivative **105** whereas the similar reduction in *p*-xylene affords **106** as shown in Scheme 26 [66]. Treatment of [$RuCl_2(tmps)(PMe_3)$] (**104**) with 2 equiv. of either Me_3SiCH_2MgCl or Me_3CCH_2MgCl in THF affords novel ruthanacyclobutane complexes **108** and **109**, respectively [67]. Similarly, the analogous complex **107** was obtained in an NMR tube reaction of **104** with Me_3CCD_2MgBr. The four-membered metallacyclic ring is planar without any interaction between the metal center and the ring-bound methyl groups as revealed by the single crystal X-ray structure of **109**. The molecule resembles the analogous complex, [$(Me_3P)_4Ru(\eta^2$-$CH_2CMe_2CH_2)$] prepared from $(Me_3CCH_2)Mg$ and $Ru_2(OAc)_4Cl$ in the presence of PMe_3 [68]. The thermolysis of **109** in toluene at 75 °C produces a mixture of *endo* (**110**) and *exo* (**111**) isomers of [$(tmps)(Me)Ru(\eta^3$-$CH_2CMeCH_2)$] in quantitative yield [69]. The above complex can also be synthesized by direct reaction of [$(tmps)(Me_3P)(Me)RuCl$] (**113**) with $CH_2{=}CMeCH_2$-$MgBr$ in diethyl ether. Interestingly, the kinetic investigation has indicated the β-methyl transfer in the presence of excess of phosphine indicating the reversibility of this process. The details are summarized in Scheme 27. This is the first example a the direct observation of a reversible β-methyl elimination or migratory insertion in a metal complex (**109**). This kind of β-migratory insertion is well documented as a fundamental carbon–carbon bond forming process that is vital to metal-catalyzed dimerization, oligomerization and polymerization similar to Zeigler–Natta polymerization systems.

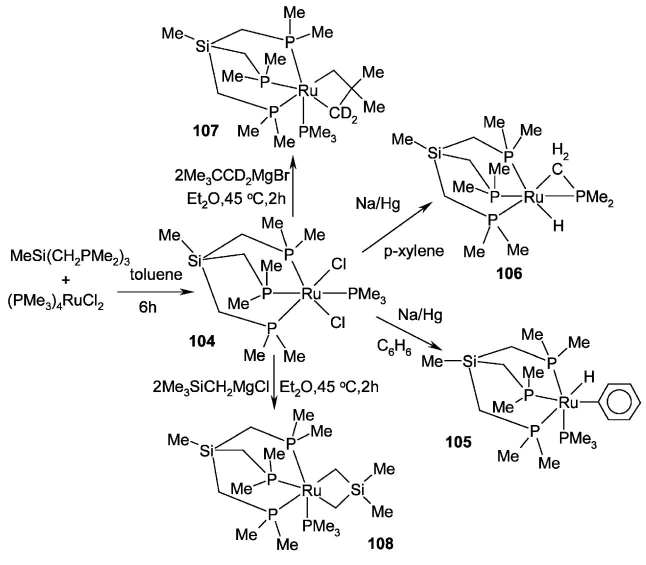

Scheme 26.

Complex **104** on treatment with $LiBEt_3H$ yields hydridochloride complex **115** in 36% yield. The reaction of **104** with $LiAlH_4$ affords the corresponding dihydride complex **116**, which on addition of 1 equiv. of NH_4BPh_4 yields the ammonia complex **117** in good yield. Treatment of **115** or **117** with strong base such as KOBu or $KN(SiMe_3)_2$ led to the formation of the internally cyclometalated complex **118** in 70% yield through C–H activation of one of the methylene bridges in the triphos ligand. The structure of the cyclated product **118** was confirmed by an X-ray diffraction study. The molecule possesses a strongly distorted octahedral geometry without substantial elongation of Ru–P bonds as expected. The Ru–C bond distance is 2.282(6) Å.

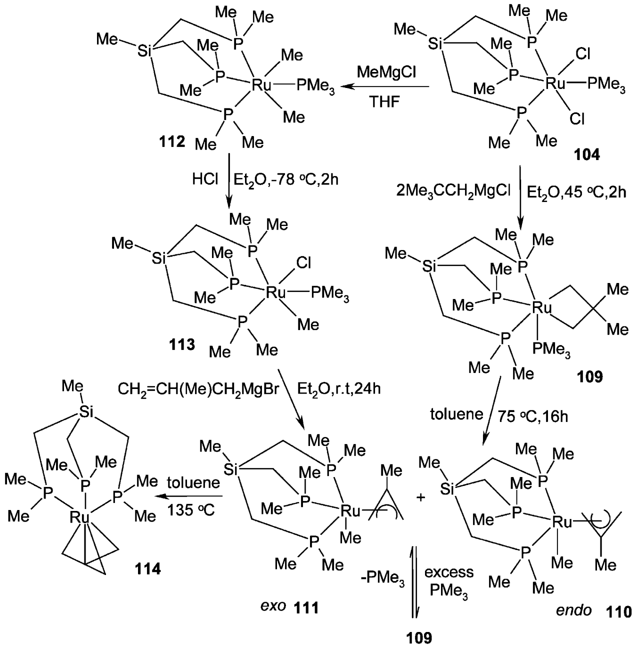

Scheme 27.

Further reactions of **115** with a variety of organic substrates are described in Scheme 28 [70].

Reaction of $MeHSi(CH_2CH_2CH_2PPh_2)_2$(biPSiH) with *mer*-$RuH(PPh_3)_3(CO)Cl$ afforded a bright yellow air-stable solid, which on further exposure to gaseous CO gave a mixture of five-coordinate monocarbonyl ruthenium(II) complex, [Ru(biPSi)(CO)Cl] (*syn*, **125**; *anti*, **126**) and six-coordinate dicarbonyl complex, $[Ru(biPSi)(CO)_2Cl]$ (**127**) as shown in Scheme 29. The structures of both the complexes (*syn*, **125** and **127**) were confirmed by X-ray diffraction studies [71]. The complex **125** adopts a distorted trigonal-bipyramidal geometry. Although, the biPSi cage is coaxial, all the equatorial angles are different from each other and from 120°. The X-ray structure of complex **127** confirms two carbonyl groups in mutually *trans* orientation; the unit cell contain two independent molecules that differ from one another only in the conformational relationship of the biPSi methylene backbone similar to that found in osmium complex, *cis*-$[Os(CO)_2(PPh_2CH_2CH_2SiMe_2)]$ [72]. The reaction of biPSiH with $[Ru(PPh_3)_2(CO)_3]$ affords $[RuH(biPSi)(CO)_2]$ in quantitative yield as a mixture of *syn* diastereomer **128** and its *anti* analogue **129** as shown by X-ray crystallography. Subsequent treatment of **128** with CCl_4 then $LiAlH_4$ leads to the formation of $[RuH(biPSi)(CO)_2]$ (**130**) (Scheme 30) [73].

The complex **128** reacts slowly with either wet piperidine or molecular oxygen to afford novel silaxo complexes **133** and **134**. The exchange of CO with ^{13}CO (1 atm) at r.t. is extremely slow and so is the substitution of the CO groups. The ligand substitution at d^6 Ru(II) center requires forcing conditions. The substitution of

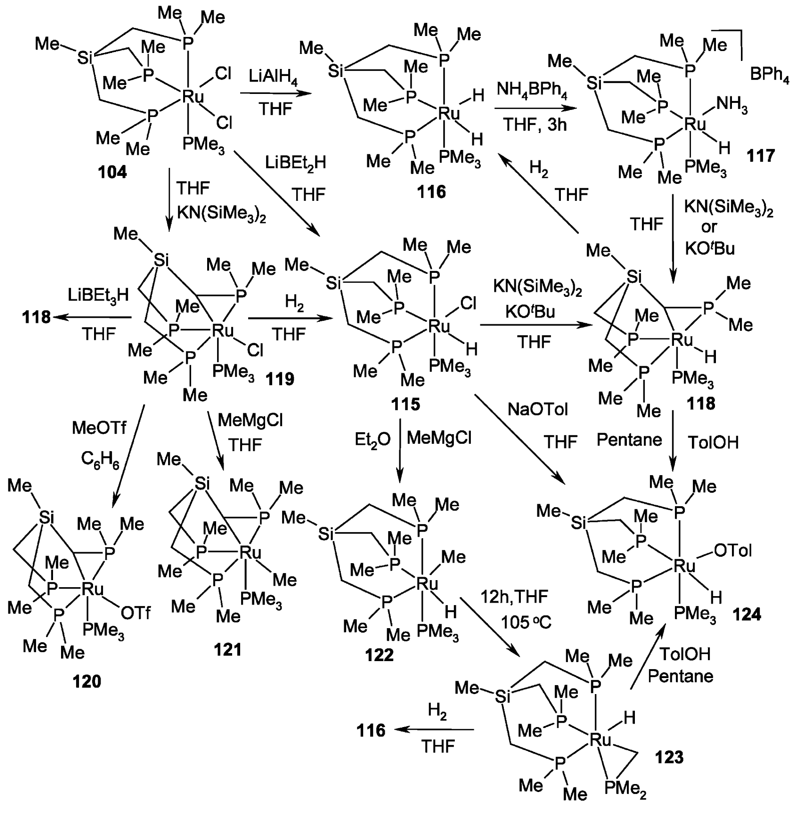

Scheme 28.

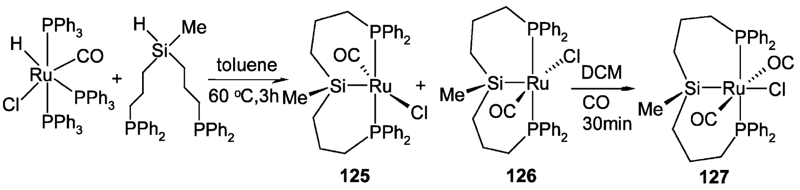

Scheme 29.

CO by $P(OMe)_3$ occurs *trans* to the strongly labilizing silyl group only after refluxing in toluene for 2 h. Although, the complex **136** is stable to air in the solid state, refluxing the benzene solution for more than 7 days, leads to insertion of oxygen into both the Ru–Si and Si–Me bonds to give the complex **134** as described in Scheme 30. Addition of $P(OMe)_3$ gives a diastereomeric derivative **137**; the major isomer was selectively crystallized from diethyl ether and the structure was determined by X-ray diffraction studies [74].

Sealed tube reactions of bis(phosphino)alkylsilane, $MeSiH\{(CH_2)_nPPh_2\}_2$ ($n = 2$ or 3) with $Ru_3(CO)_{12}$ afford mononuclear dicarbonyl complexes **138** and **139** with Si–Ru σ-bond anchored with attachment of the *trans* phosphorus atoms at the ruthenium center [75]. The structure of the complex **139** is confirmed by a single crystal X-ray analysis which depicts the octahedral geometry about ruthenium(II) where the two carbonyl groups are *cis* and the tridentate ligand framework is *mer*; the H atom occupies the sixth site with a *syn* disposition with respect to the methyl group at the silicon center. The silyltris(phosphine), $MeSi(PR_2)_3$ reacts with $Ru_3(CO)_{12}$ to give $[Ru_3(CO)_9\{MeSi(PR_2)_3\}]$ (**140**–**142**) (Scheme 31) [76]. The tridentate ligand caps the triangular array of ruthenium atoms and makes the cluster resistant to dissociation under Fischer–Tropsch catalytic reaction conditions [23]. The reaction of $[Ru(COD)\{\eta^3\text{-}(CH_2)_2CMe\}_2]$ with bis(phosphinoalkyl)silane, $Me_2Si(CH_2PPhR)_2$ (R = 1-Np, R = *o*-An) gives chelate complexes **143** and **144** with the elimination of olefin. These complexes were effectively used as enantioselective hydrogenation catalysts [77]; the details are given in Section 5. The stereogenic ligand $Me_2Si[CH_2P(1\text{-}Np)(Ph)]_2$ reacts with $[RuCl_2(PPh_3)_3]$ in toluene at r.t. to give the dark red microcrystalline complex **145** in 89% yield (Scheme 32).

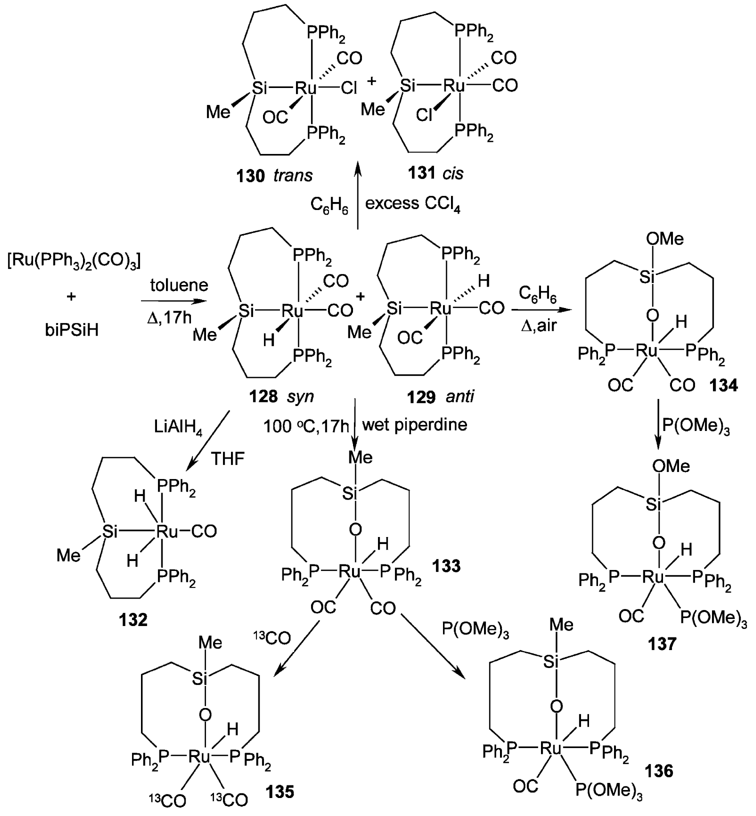

Scheme 30.

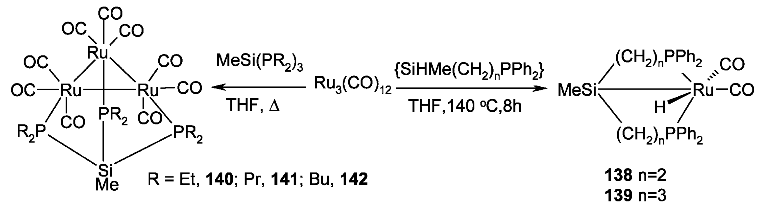

Scheme 31.

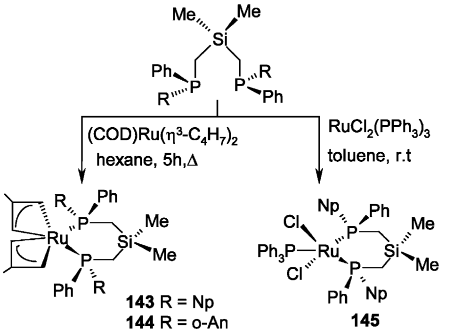

Scheme 32.

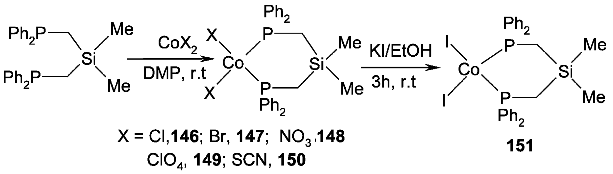

Scheme 33.

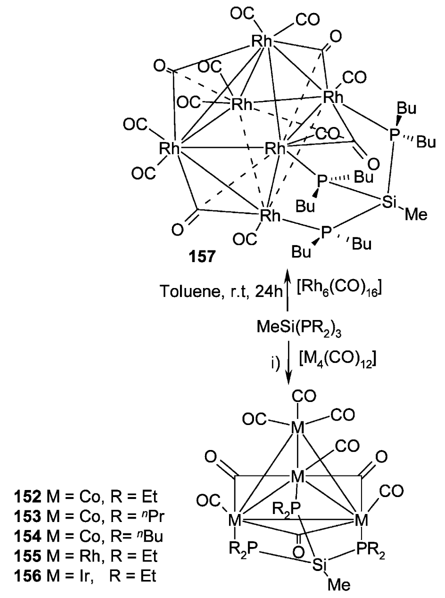

i) M = Co, hexane, r.t, 15h;M = Rh, hexane, r.t, 15h;
M = Ir, THF, Me$_3$NO.2H$_2$O

Scheme 34.

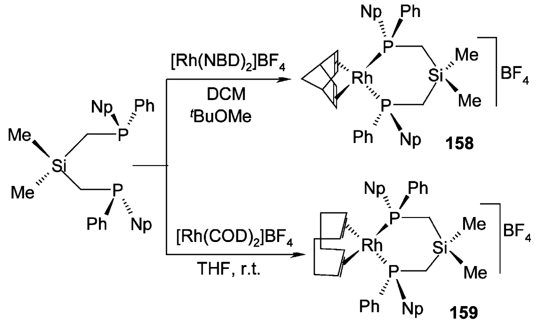

Scheme 35.

3.8. Group 9

The bidentate phosphine ligand, $Me_2Si(CH_2PPh_2)_2$ forms a series of cobalt(II) complexes of general formula $[CoX_2\{Me_2Si(CH_2PPh_2)_2\}]$ (**146**–**151**) (X = Cl, Br, I, NO_3, ClO_4, NCS) which are characterized by electronic and infrared spectroscopic data and by magnetic moment studies (Scheme 33). The X-ray structure determination of the bromo derivative, $[CoBr_2\{Me_2Si(CH_2PPh_2)_2\}]$ (**147**) reveals a tetrahedral geometry at the cobalt center with the ligand exhibiting a bite angle of 101.54(6)° [78].

The tridentate phosphine, $MeSi(PR_2)_3$ (R = Et, ^{n}Pr, ^{n}Bu) reacts with $Co_4(CO)_{12}$ in hexane at r.t. to form $[Co_4(CO)_9\{MeSi(PR_2)_3\}]$ (**152**–**154**) in which the tridentate ligand caps a carbonyl-bridged triangular face of the metal tetrahedron [79]. The spectroscopic data for these complexes indicate that the structures are analogous to those proposed for tripod ligand derivative of the type $[M_4(CO)_9\{HC(PPh_2)_3\}]$ (M = Co, Rh) [80]. Similar reactions of $Rh_4(CO)_{12}$ or $Ir_4(CO)_{12}$ with $MeSi(PEt_2)_3$ leads to the formation of $[M_4(CO)_9\{MeSi(PEt_2)_3\}]$ (M = Rh, **155**; Ir, **156**). In the case of the iridium derivative, a better yield is obtained by carrying out the reaction in THF in the presence of an equimolar quantity of TMNO [79]. The tridentate ligand $MeSi(PBu_2)_3$ reacts with $Rh_6(CO)_{16}$ in toluene to yield $[Rh_6(CO)_{13}\{MeSi(PBu_2)_3\}]$ (**157**) in very low yield (Scheme 34).

The diphosphine, (*S*,*S*)-$Me_2Si[CH_2P(1\text{-}Np)(Ph)]_2$ containing stereogenic phosphorus atoms reacts with $[Rh(olefin)_2]BF_4$ (olefin = NBD or COD) to give the ionic complexes **158** and **159** in good yield (Scheme 35) [23].

The diolefin complex, $[Rh_2Cl_2(NBD)_2]$ on treatment with silver triflate, gives the solvated intermediate $[Rh(NBD)(S)_2]^+$ (S = acetone or acetonitrile) which

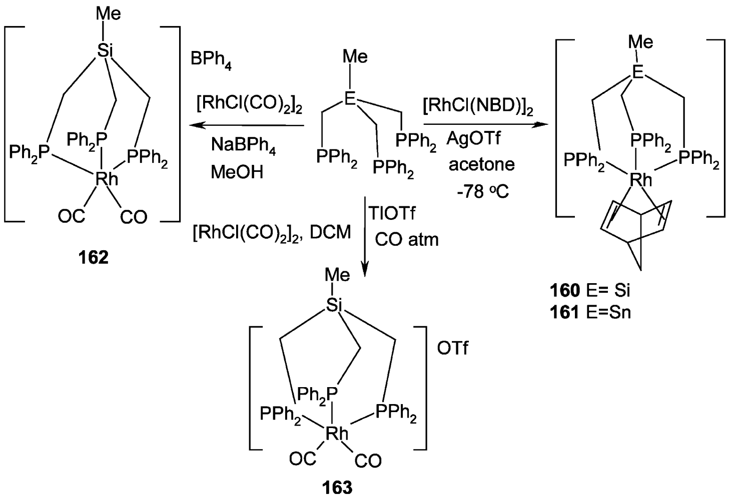

Scheme 36.

then reacts with Si-triphos, $MeSi(CH_2PPh_2)_3$ to give complex **160** in quantitative yield. The analogous Sn-triphos, $MeSn(CH_2PPh_2)_3$ also yields the similar complex **161**. The X-ray structures of both the silicon and tin complexes reveal a distorted trigonal-bipyramidal geometry around rhodium with one olefinic bond and one phosphorus atom being axial and the remaining two phosphorus atoms and the other olefin bond constituting the equatorial plane. The reaction of Si-triphos with $[RhCl(CO)_2]_2$ in methanol under a CO atmosphere in the presence of $Na[BPh_4]$, silver or thallium triflate affords the corresponding cationic dicarbonyl complexes $[Rh(CO)_2(Si\text{-triphos})]^+$ as shown in Scheme 36. The above method of preparation also gives the analogous Sn-triphos complex, $[Rh(CO)_2(Sn\text{-triphos})]^+$ [31].

The reaction of $HSi(CH_2CH_2PPh_2)_3$ (triPSiH) with $[Rh(COD)Cl]_2$ affords the six-coordinate rhodium(III) complex [Rh(triPSi)H(Cl)] (**164**) which on treatment with $SnCl_2$ in THF gives a trichlorostannyl derivative $[Rh(triPSi)H(SnCl_3)]$ (**165**). Addition of MeLi (in excess of diethyl ether) or $NaN(SiMe_3)_2$ (in excess of THF) to a THF solution of **164** containing excess of $LiAlH_4$ under a CO atmosphere affords the bright-lemon colored five-coordinate rhodium(I) complex [Rh(triPSi)(CO)] (**166**) as shown in Scheme 37. The structure of **166** was determined by X-ray crystallography [81]. In a rhodium-$MeSi[CH_2CH_2PPh_2]_3$ catalyzed hydroformylation of 1-butene the same complex **166** was obtained in low yield; the first Rh(I)–Si bonded complex to be characterized and reported [82]. The trigonal-bipyramidal complex **166** was formed via an unusual rhodium-promoted carbon–silicon bond cleavage, which removes the methyl group from the ligand. The methyl group is presumably converted to methane by reductive elimination from a rhodium methyl hydride intermediate. Similar carbon–silicon bond cleavage in tetraalkyl silanes was previously observed in the presence of trichlorosilane and chloroplatinic acid [83].

The reaction of $MeSiH\{(CH_2)_3PPh_2\}_2$ with $[Ir(COD)Cl_2]$ affords complex **167** in excellent yield. Interestingly, the reaction between $MeSiH\{(CH_2)_3PPh_2\}_2$ and *trans*-$[M(PPh_3)_2(CO)Cl]$ afforded a mixture of two stereoisomers **168** and **169** in 3:1 ratio as revealed by NMR spectroscopic data. When this mixture is treated with tin(II)chloride in THF solution afforded an iridium–tin complex, $[IrH(CO)SnCl_3\{MeSi\{(CH_2)_3PPh_2\}_2\}]$ as another pair of stereoisomers **170** and **171** in the same 3:1 ratio. Surprisingly, the minor isomer **171** crystallized preferentially giving X-ray quality crystals; the structure confirms an octahedral iridium(III) geometry in which H and CO are *trans* to one another and the distorted trichlorostannyl ligand occupies a site *trans* to the silicon of the tridenate framework. Treatment of the same isomeric mixture with $LiAlH_4$ in THF afforded a mixture of isomers of the dihydride, $[IrH_2\{MeSi\{(CH_2)_3PPh_2\}_2\}(CO)]$ (**172**–**175**) as shown in Scheme 38 [75]. The reaction of $HSi(CH_2C_6H_4PPh_2\text{-}o)_3$ with $[Ir(COD)Cl]_2$ leads to the oxidative addition at the metal center to give an hydride complex, $[IrH\{Si(CH_2C_6H_4PPh_2\text{-}o)_3\}Cl]$ (**176**) in quantitative yield (Eq.

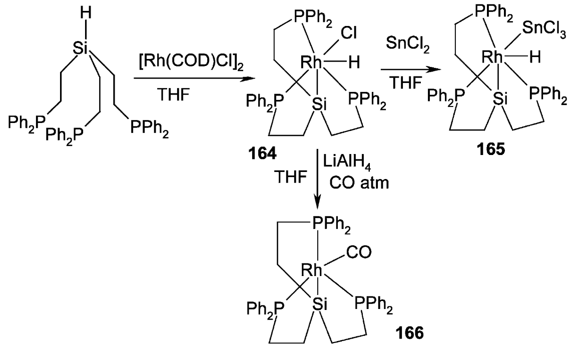

Scheme 37.

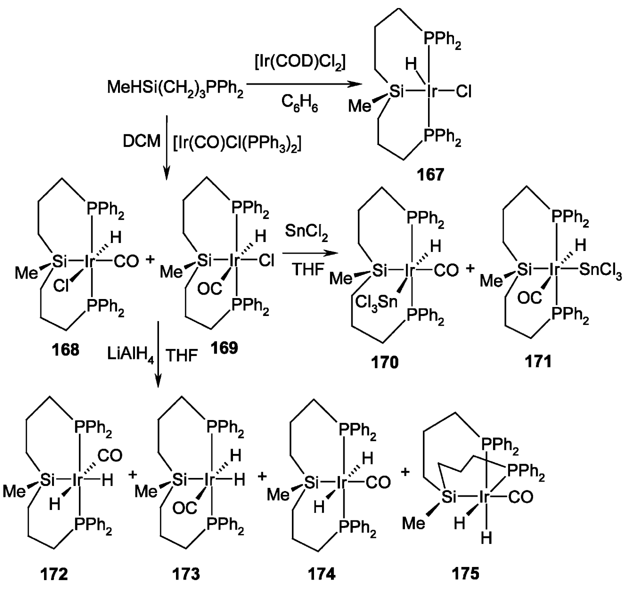

Scheme 38.

(10)) The structure and formulation were confirmed by NMR studies [16].

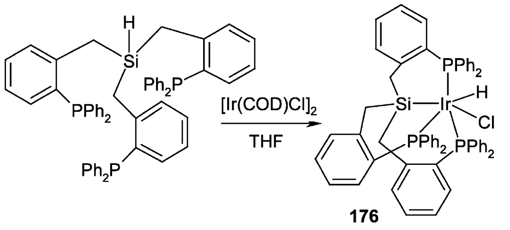

(10)

3.9. Group 10

The first nickel(II) complex of silylalkylphosphine was reported by Alyea and coworkers [84]. The reaction of nickel(II) nitrate with $Me_2Si(CH_2PPh_2)_2$ gave orange and violet crystals of $[Ni(NO_3)_2\{\eta^2\text{-}Me_2Si(CH_2PPh_2)_2\}]$ (**177**) which is the first example of a nickel(II) nitrate containing a ditertiary phosphine. The complex **177** is on the square-planar⇔tetrahedral threshold. The structure of orange isomer was confirmed by a single crystal X-ray analysis. The geometry at the nickel atom is slightly distorted square-planar towards square-pyramidal; the six-membered chelate ring adopt a boat conformation. Reaction of silylalkylphosphine, $Me_2Si(CH_2PPh_2)_2$ with $NiCl_2$ in the ethanol affords chelate complex, $[NiCl_2\{\eta^2\text{-}Me_2Si(CH_2PPh_2)_2\}]$ (**178**) in good yield. The reaction of $Me_2Si(CH_2CH_2PPh_2)_2$ with $[PdCl_2(NCMe)_2]$ affords the expected *cis*-chelate complex **179** as shown in Scheme 39 [50].

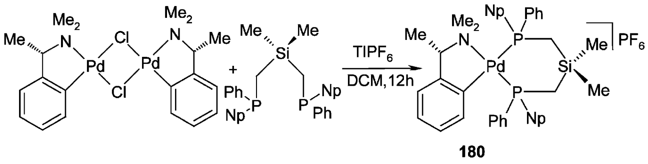

(11)

The reaction of $Me_2Si[CH_2P(1\text{-}Np)(Ph)]_2$ with bis(μ-chloro)bis{(*S*)dimethyl(1-methylbenzyl)-aminoato-*C*,*N*}dipalladium(II) in methanol in the presence of $TlPF_6$ gives a mononuclear complex **180** as shown in Eq. (11) [23]. The corresponding (*R*)-isomer was prepared analogously. The enantiomeric purity of the diastereomers is determined by integration of the ^{31}P-NMR spectrum. Addition of $RSiH\{(CH_2)_nPR'_2\}_2$ to $[PtCl_2(COD)]$ in the presence of NEt_3 affords square-planar complexes **181**–**187** with a Si–Pt bond; cleavage of the

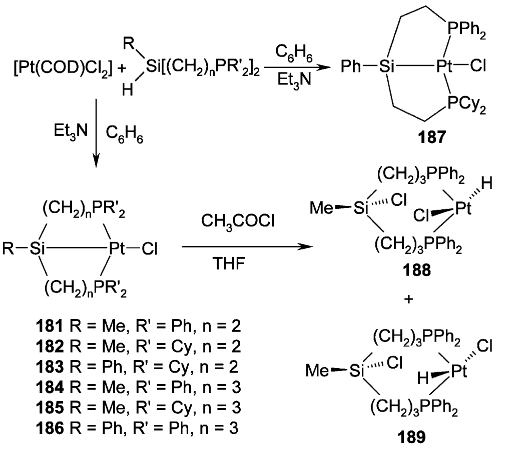

Scheme 40.

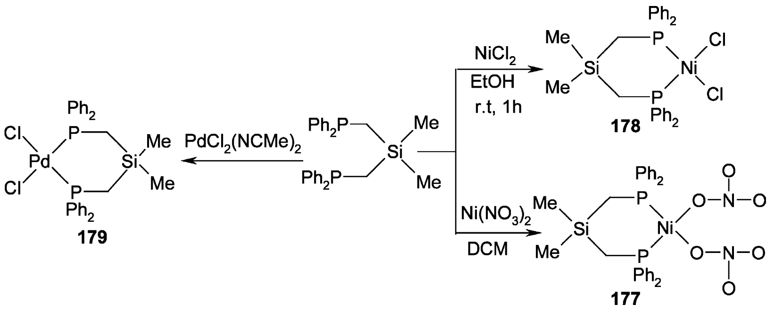

Scheme 39.

Si–Pt bond by MeCOCl affords a pair of diastereomers (**188** and **189**) in which the two P centers are disposed in a *trans* fashion (Scheme 40). Analogous complexes with improved solubility were obtained by introduction of cyclohexyl groups in place of phenyl groups at the phosphorus centers. Improved solubility was also observed when the number of backbone methylenes was increased from two to three. The crystal structure of **184** was determined by X-ray analysis; the angles between the four ligating atoms at the platinum center are all very close to 90° suggesting a square-planar geometry around the platinum(II) center [75].

The reaction of silylbis(phosphine), MeHSi(CH_2-$C_6H_4PPh_2$-*o*)$_2$ with Pt(COD)Cl_2 in dichloromethane affords [Pt{MeSi($CH_2C_6H_4PPh_2$-*o*)$_2$}Cl] (**190**) by elimination of HCl as shown in Eq. (12). The structure and formulation were confirmed by NMR studies [16].

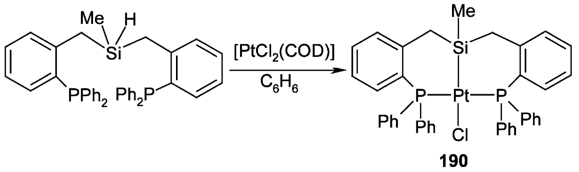

(12)

The reaction between [$PtCl_2(PPh_2OH)_2$] and Cl_2SiPh_2 yields the platinum silyldiphosphinite complex **191** as shown in Eq. (13), was confirmed by single crystal X-ray analysis [85]. The platinum shows a typical square-planar geometry with silyldiphosphinite showing *cis*-chelation with a bite angle of 96.7°.

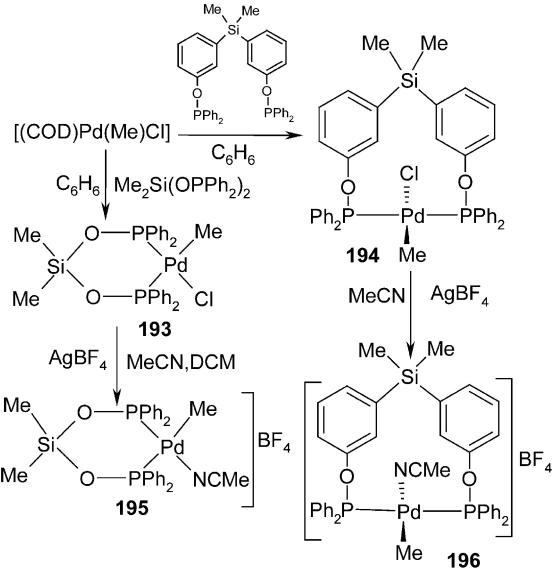

Scheme 41.

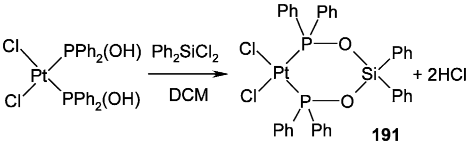

(13)

Dixon and Rattray have reported the reaction of [PtCl(PEt_3){($PPh_2O)_2$H}] with Me_3SiCl and predicted the product as an ionic complex **192** (Eq. (14)). However, they were inconclusive about the structural formulation as further attempts to purify the product led to the formation of very insoluble products [86].

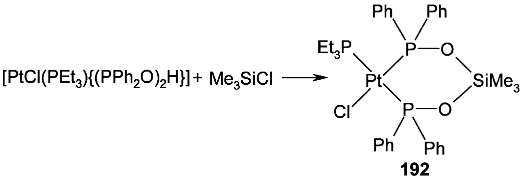

(14)

The reaction of [Pd(COD)MeCl] with silyldiphosphinites, $Me_2Si(OPPh_2)_2$ and $Me_2Si(OC_6H_4PPh_2$-*m*)$_2$ affords *cis* (**193**) and *trans* (**194**) complexes, respectively, as shown in Scheme 41 [87]. These complexes were prepared in order to explore their catalytic ability in the copolymerization of ethylene and CO. The details are given in Section 5.

3.10. Group 11

Group 11 chemistry of silylbis- and silyltris(phosphines) is yet to be explored. However, Alyea and coworkers have reported [88] the first and the only example of a copper–silylmonophosphine complex **197** obtained by reacting $CuBr_2$ with 2 equiv. of $Ph_2PCH_2Si(CH_3)_2CH{=}CH_2$; the complex is dimeric in nature with the ligand exhibiting a bidentate mode of coordination (Eq. (15)). The X-ray structure of **197** reveals the dimeric nature of the complex. The metal is a five coordinate, an 18-electron center with copper atoms bridged by bromine atoms.

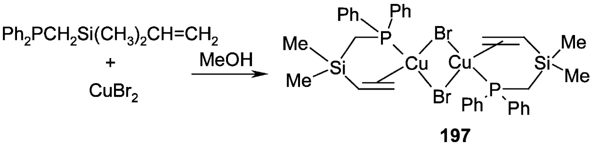

(15)

3.11. Group 12

Reactions of bis(phosphinoalkyl)silane, $Me_2Si(CH_2$-$PPh_2)_2$ with zinc and cadmium chlorides yield pseudotetrahedral metal complexes. Alyea and co workers have reported the preparation of a zinc [50] complex (**198**)

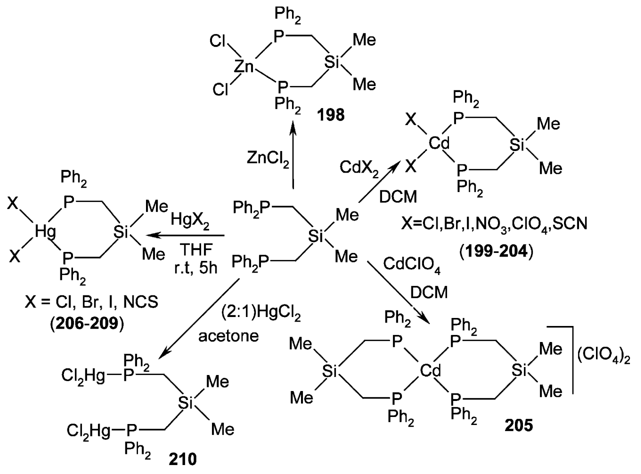

Scheme 42.

and a series of cadmium complexes [89] of general formula $[CdX_2L_2]$ (**199**–**204**) (X = Cl, Br, I, NO_3, ClO_4, NCS; $L = Me_2Si(CH_2PPh_2)_2$). Reaction between $[Cd(ClO_4)_2]$ and 2 equiv. of ligand affords the bis-chelated complex **205** in 70% yield. The structure of **199** was determined by single crystal X-ray studies. The complex is tetrahedral in nature with a bidentate phosphine ligand exhibiting a bite angle of 101.54(6)°. The same ligand reacts with mercury(II) salts to form chelate complexes of general formula $[HgX_2L]$ (**206**–**209**) (X = Cl, Br, I, NCS). Addition of 2 equiv. of $HgCl_2$ to the same ligands results in the formation of $[(HgCl_2)_2(\mu\text{-}Me_2Si(CH_2PPh_2)_2]$ (**210**) in which the silylphosphine exhibits a bridged bidentate mode of coordination (Scheme 42).

All complexes were characterized by NMR and IR spectroscopic data as they are soluble in organic solvents unlike most of the complexes of mercury(II) salts. The ^{31}P-NMR spectra of the mercury complexes show single resonances with characteristic $^1J_{PHg}$ values. The magnitude of $^1J_{PHg}$ varies in the order $Cl > Br > SCN > I$ similar to the monosilylphosphine analogues [90]. Further, the $^1J_{PHg}$ values vary significantly for monomeric and dimeric species and the dimeric complexes show very large values. The $^1J_{PHg}$ coupling constant is correlated with the Hg–P distance, X–Hg–X and P–Hg–P bond angles, the ionization potential of X and the 6s(Hg)/3s(P) orbital overlap. The structure of the iodide derivative **208** was determined by a single X-ray study. The mercury center exhibits tetrahedral geometry with the ligand bound in a bidentate chelating fashion. The silyldiphosphinite, $Me_2Si(OPPh_2)_2$ reacts with $HgBr_2$ to give the chelate complex $[HgBr_2\{Me_2Si(OPPh_2)_2\}]$ (**211**) in quantitative yield [27].

4. Reactions of related phosphines

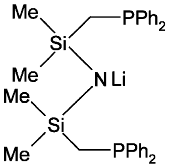

XIII

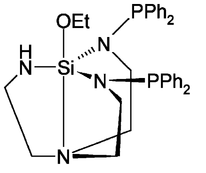

XIV

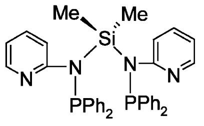

XV

Fryzuk and coworkers [91–93] have extensively studied the coordination chemistry of a novel nitrogen bridged heterofunctional bis(phosphine), $LiN\{Si(Me_2)CH_2PPh_2\}_2$ containing two organosilicon spacers along with two methylene groups in the backbone. Another interesting and novel ligand, ethoxy-*N*,*N′*-bis(diphenylphosphino)azasilatrane, $(EtOSi(Ph_2PNCH_2CH_2)_2(HNCH_2CH_2)N)$ derived from azasilatranes was developed by Verkade and coworkers [94]. This derivative behaves similar to bis(tertiaryphosphines) and thus allows facile alkylation, oxidation with sulfur and also complexation. The coordination chemistry of this compound is interesting as it show two different coordinating modes with the transition metals, either as a bidentate (*P*,*P′* coordination) or tridentate (*P*,*P′*and *O* of ethoxy coordination) ligand.

Woollins and coworkers have reported [24] a diphosphine, $Me_2Si[N(C_5H_4N\text{-}2)PPh_2]_2$ (**XV**) with a PNSiNP framework which was prepared by reacting 2-(diphenylphosphinoamino)pyridine with LiN^iPr_2 followed by the addition of dimethyldichlorosilane. The bis(phosphine) forms *cis*-chelated complexes with palladium(II) (**212**) and platinum(II) (**213**) derivatives; the solution of which on exposure to moisture hydrolyses to give cationic complexes (**214**) as shown in Scheme 43. This may be due to the labile nature of the N–Si bond and also the strong preference to form a stable five-membered *P*,*N* chelate complex. However, a stable platinum chelate complex **215** was obtained when the diphosphine react with $[Pt(COD)Me_2]$. The structures of the diphosphine ligand and its platinum derivatives **214** and **215** are established by single crystal X-ray analysis.

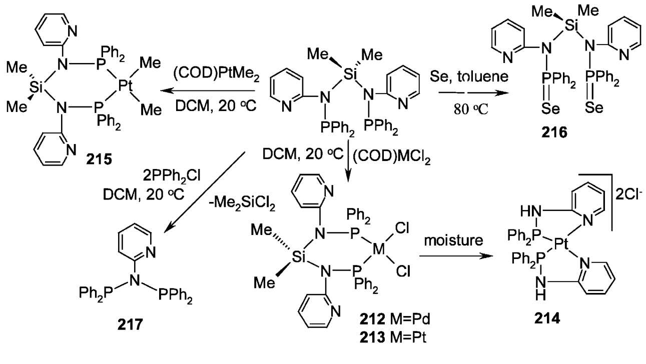

Scheme 43.

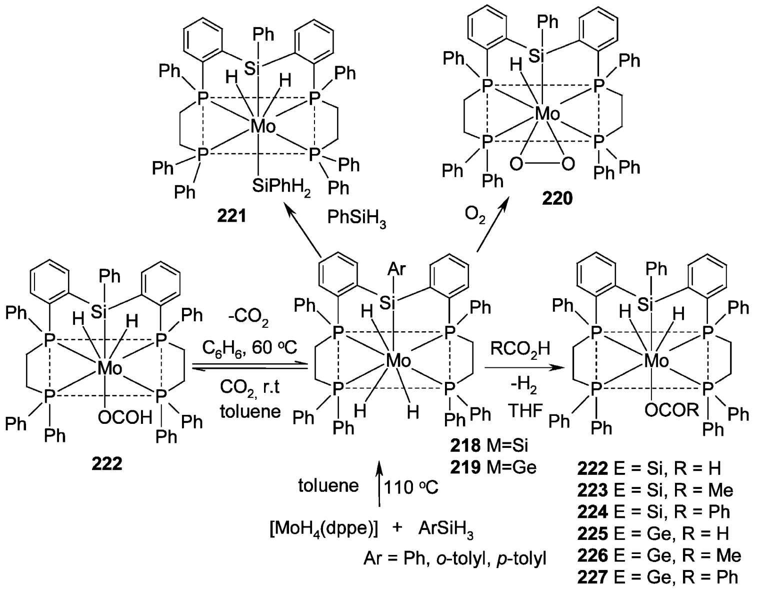

Scheme 44.

The diselenide derivative **216** was prepared by reacting diphosphine with 2 equiv. of elemental selenium in dichloromethane. Further, the compound reacts with 2 equiv. of PPh_2Cl in dichloromethane at 20 °C to give 2-pyridylaminobis(diphenylphosphine) (**217**) with the elimination of dimethyldichlorosilane.

The thermal reaction of $[MoH_4(dppe)_2]$ with $PhSiH_3$ affords an unusual complex **218** containing a quadruply chelated silylphosphine ligand as shown in Scheme 44. Similar reaction with $PhGeH_3$ gives the analogous germyl complex **219** [95,96]. The formation of the complex is novel since it involves activation not only of a Si–H or Ge–H bond but also two C–H bonds of the *ortho* positions of the phenyl groups in the dppe ligands simultaneously. In addition the complex can show interesting reactivity because of an almost open coordination site available at the axial position opposite to the Si atom, which can also exert a strong *trans*-effect. The complex **218** reacts with O_2 to give the unprecedented Mo(IV) peroxo type η^2-O_2 complex **220** as shown in Scheme 44, was confirmed by X-ray diffraction study [97]. The quadruply chelated silyl and germyl–molybdenum complexes on treatment with 2 equiv. of carboxylic acid (formic acid, acetic acid or benzoic acid) in THF at r.t. afford monocarboxylato molybdenum complexes **222**–**227** in 70–90% yield (Scheme 44). The structure of **222** has been established by single crystal X-ray analysis. Maintained a toluene solution of **218** under CO_2 (17 atm) at r.t. gives **222** in 82% yield; interestingly, benzene solution of this species on warming revert back to **218** with the evolution of CO_2. This remarkable reversible insertion of CO_2 into the Mo–H bond under mild conditions is explored in CO_2 fixation reactions. In a typical reaction, a toluene solution of **218** was allowed to react under CO_2/H_2 (25/35 atm) pressure in the presence of dimethylamine at 110 °C to afford 115 equiv. of *N*,*N′*-dimethylformamide with respect to the complex **218**. The reaction of **218** with an excess of 2,4-pentanedione in toluene under refluxing conditions affords complexes **228** and **229**; the structural formulation of which is based on spectroscopic data and X-ray crystallographic analysis of **228** [98]. The X-ray analysis shows the existence of both chelating and monodentate dppe ligands along with the η^2-2,4-pentanedionato ligand. When the trihydrido complex **218** was treated with excess of dialkyl malonates $CH_2(COOR)_2$ (R = Et, ^{i}Pr, ^{n}Pr, CH_2Ph) in toluene under refluxing conditions, complexes **230**–**233** were obtained in around 50% yield. The details are summarized in Scheme 45.

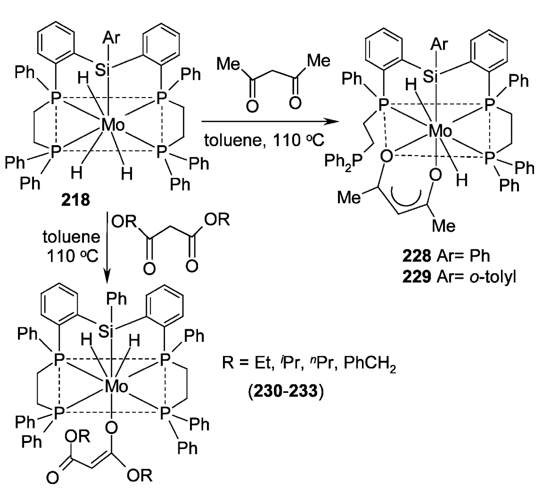

Scheme 45.

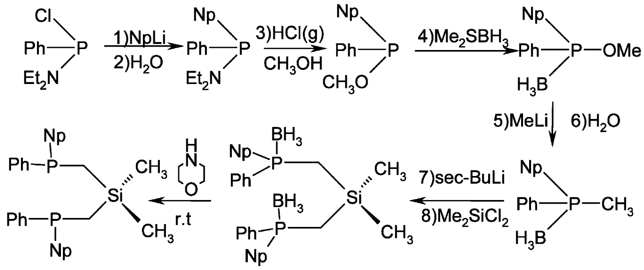

Scheme 46.

5. Catalytic applications

Enantioselective catalysis by chiral phosphines is well documented. The diphosphine BIPNOR containing stereogenic phosphorus atoms has been successfully used in enantioselective catalysis and this has given potential diphosphines containing stereogenic phosphorus atoms a new dimension in enantioselective catalysis. However, the lack of availability of easier synthetic methodologies and bulk synthesis, the low solubility and the stability of the configuration have limited their use in such applications. Juge and co-workers [96] with an input from Imamoto [99], have reported a new strategy for the synthesis of enantiomerically pure borane-protected chiral phosphines of the type P(Ph)(R)-(Me)(BH_3) in which methyl group can be selectively lithiated. Stoop and Mezzett have reacted P(Ph)(R)-(BH_3)CH_2Li with R_2SiCl_2 to obtain P-chiral diphosphine $Me_2Si\{CH_2P(Np)Ph(BH_3)_2\}_2$ in good yield [23]. The free phosphine can be obtained by reacting with an amine to release the borane (Scheme 46).

The rhodium derivative [Rh(COD){(*S*,*S*)(PPh(Np)-$CH_2)_2SiMe_2$}]BF_4 (**159**) catalyzes the asymmetric hydrogenation of (acylamino)cinnamato derivatives with high enantio-selectivity [23]. The data are listed in Table 5. Reports of such catalytic hydrogenation of *N*-substituted enamides are rare and the best enantioselectivity does not exceed 75%.

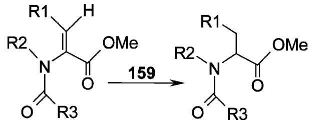

Table 5
Asymmetric hydrogenation of *Z*-1-methyl-acetamidocinnamate to (*R*)-*N*-acetylphenyalanine methylester

S. number	R^1	R^2	R^3	ee (%)	Configuration
1	Ph	H	Me	97.7	*R*
2	Ph	H	Me	97.1	*R*
3	H	H	Me	64.1	*R*
4	Ph	Me	Me	96.2	*R*
5	Ph	Me	Ph	96.5	*R*
6	Ph	Me	Ph	0	

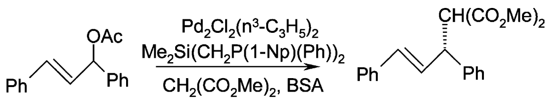

T(°C)	e.e(%)
20	27
0	10

Scheme 47.

The ruthenium(II) derivative [$RuCl_2(PPh_3)\{\eta^2$-Me_2-$Si(CH_2PPh(Np))_2\}$] catalyzes the hydrogenation of pentane-2,4-dione to (*S*,*S*)-pentane-2,4-diol with moderate enantioselectivity [23]. The reaction catalyzed by **145** is slower than with the Binap and Biphemp analogues. The silylphosphine ligand was also tested in the palladium-catalyzed substitution reaction of racemic allylic acetates by carbon nucleophiles. Racemic 1,3-diphenyl-3-acetoxypropene was treated with dimethyl malonate in the presence of insitu generated catalyst from [$Pd_2Cl_2(\eta^3$-$C_3H_5)_2$] and $Me_2Si[CH_2P(Np)Ph]_2$. The alkylation product was obtained in nearly quantitative yield after 4 h of reaction at r.t. but with low enantionselectivity (27% ee). Decreasing the reaction temperature to 0 °C lowers the enantioselectivity (10% ee) (Scheme 47).

Asymmetric hydrogenation of tiglic acid was performed employing several chiral complexes of the type [(PP)Ru(II){η^3-$(CH_2)_2CHCH_3\}_2$] where PP is a diphosphine ligand [100]. The results (given only for the complex **143** containing $Me_2Si\{CH_2PPh(C_6H_4OMe$-*o*$)\}_2$ is) clearly show that the hydrogenation proceeds smoothly to afford the 2-methyl butyric acid in quantitative yield. The enantiomeric excesses were in the range of 1–98%. The ligands with chirality at the phosphorus centers show poor enantioselectivity with the silyl derivative showing 15% whereas the diphosphine having chiral carbon centers shows remarkable results with enantioselectivity as high as 98% (Eq. (16)).

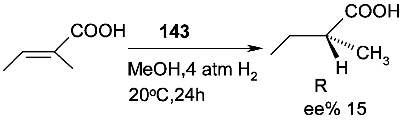

(16)

The ruthenium(II) complex **144** catalyzes the hydrogenation of penatane-2,4-dione to (*S*,*S*′)-pentane-2,4-diol with moderate enantioselectivity as shown in Scheme 48 [23]. The reaction catalyzed by **144** is

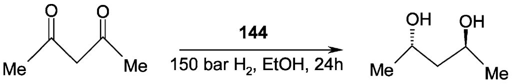

T(°C)	(S,S)	e.e.(%)	(R,S)
80	93%	56%	7%
100	91%	53%	9%

Scheme 48.

Table 6
Butene hydroformylation with mono-, di-, tri- and tetraphosphines

Ligand (L)	L/Rh	Rate (M^{-1} min^{-1})	*n*-Pentanal/total pentanal (%)	Selectivities to products (%)			
				n-Heptanal	2-Methylbutanol	2-Butene	Butane
1. $(CH_3)_3SiCH_2CH_2PPh_2$	12	330	77	67	19	8	6
2. $(CH_3)_2Si(CH_2CH_2PPh_2)_2$	6	123	86	78	12	6	4
3. $(CH_3)Si(CH_2CH_2PPh_2)_3$	4	77	90	82	9	6	3
4. $Si(CH_2CH_2PPh_2)_4$	3	41	90	83	10	6	2

generally slower than with the Binap and Biphemp analogues.

Hendriksen and coworkers [82] have used rhodium complexes containing phosphine ligands of the type $(CH_3)_{1,0}Si(CH_2CH_2PPh_2)_{3,4}$ in the hydroformylation of 1-butene to yield unusually high selectivity to the linear aldehyde product at low ligand/metal ratios of 3–4. The considerable increase in the catalytic performance when the ligand concentrations are very low clearly indicates that there is always sufficient ligand to form the preferred $HR(CO)L_3$ complex with no necessity to form a dimeric species. Also, the trend in the rates of reaction shows an approximate two-fold decrease in rate with each additional phosphorus center in the ligand at constant phosphine concentration. Pruett [101] have shown that the rate of hydroformylation using monophosphines decreases with increase in the concentration of the phosphines. Although, the tri and tetraphosphine ligand used in this investigation do not prefer chelation due to longer bridge length they coil around rhodium to promote chelation. The results are summarized in Table 6.

Several silylmonophosphine ligands have also been used in catalysis. Farrell et al. have examined several rhodium complexes of silylmonophosphines as catalysts in the hydroformylation of hex-1-ene [102]. The results are summarized in Table 7. The product distributions were nearly identical in the case of PPh_3 and $Ph_2PCH_2SiMe_3$ complexes. The chloro complexes have yielded better conversions than the analogous iodo complexes. This is not unusual since in the hydroformylation of pent-1-ene, $RhI(CO)(PPh_3)_2$ is known to give lower conversions.

$$CH_3CH_2CH{=}CH_2 + CO + H_2 \overset{cat.}{\rightarrow} CH_3CH_2CH_2CH_2CHO$$

$$cat. = Rh(CO)_2(acac) + Me_{4-n}Si(CH_2CH_2PPH_2)\quad (n = 1\text{–}3)$$

$$CH_2{=}CH(CH_2)_3CH_3 + CO + H_2 \overset{Catalyst}{\rightarrow} CH_3(CH_2)_4CH_2CHO + (CH_3)_2(CHCHO)(CH_2)_2CH_3$$

Several nickel complexes containing large bite bis(phosphines) were used as catalysts for hydrocyanation of styrenes (Eq. (17)). The results were remarkable with high yields and selectivity. Although, an increase in bite angle increased the yield, the ligands with bite angles in the range of 105–106° was found to be very effective for this process. The results clearly show that the effectiveness of the catalysts increases if the phosphine enhances the reductive elimination step by providing tetrahedral geometry at the metal center. Bis(phosphines) with angles of ca. 106° allow very high conversion and selectivity in the hydrogenation of styrene [103,17]. Similarly, the effect of bite angles is described in rhodium-bis(phosphine) catalyzed hydroformylation reactions [104] (Scheme 49).

Table 7
Production distribution obtained for the hydroformylation of hex-1-ene catalyzed by following complexes

Catalyst [a]	Yield (%) [b]				
	Hex-1-ene	*n*-$C_7H_{14}O$	*i*-$C_7H_{14}O$	Other	*n*/*i* [c]
$RhCl(CO)(PPh_3)_2$	0.6	61.2	35.0	3.2	1.8
$RhCl(CO)(PPh_2CH_2SiMe_3)_2$	1.7	64.2	32.6	1.2	2.0
$RhI(CO)(PPh_2CH_2SiMe_3)_2$	4.1	34.7	54.8	6.4	0.6
$RhI(CO)(PPh_2(CH_2)_3SiMe_3)_2$	74.6	18.9	4.1	2.4	4.6
$RhI(CO)(L)_2$ [d]	52.7	28.8	12.2	6.3	2.4

[a] Reactions were carried out at 100 °C and 1000 psi pressure of CO/H_2 (1/1) in an autoclave for 3 h. The molar ratio of olefin to rhodium was ca. 1000/1.

[b] Yield determined by gas chromatographic analysis.

[c] A small amount of *cis*/*trans* hex-2-ene was identified with the products.

[d] The ligand L is $Ph_2PCH_2Si(Me)(OSiMe_2)_3O$.

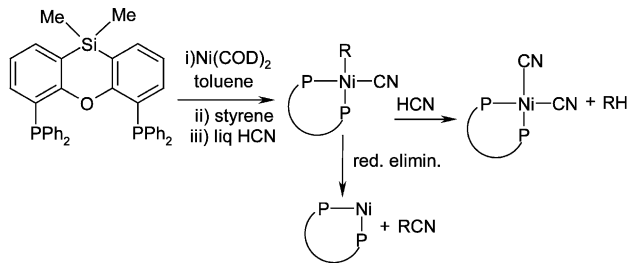

Scheme 49.

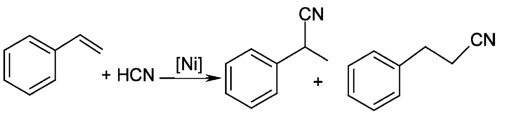

(17)

The palladium(II) neutral complexes **193** and **194** described in Scheme 41 were found to be inactive towards ethylene–CO mixture. However, after a halide abstraction with $AgBF_4$ in the presence of CH_3CN they proved to be efficient copolymerization catalysts. The catalytic reaction was carried in dichloromethane under a constant pressure of 60 bar of a 1:1 ethylene–CO mixture at 60 °C. The results of the copolymerization reactions are given in Scheme 50. It was found that the preference for *cis*- or *trans*-coordination depends on the chelate ring size. In complexes with up to 11-membered chelates, a *cis*-fixation of the ligands is observed, whereas bigger chelates afforded catalytically inactive *trans*-complexes [87].

6. Conclusions and perspectives

Although, the phosphorus–silicon bonds are generally sensitive to air and moisture; the review describes different avenues to incorporate organo-silicon moieties into the bis- or tris(phosphine) backbones to generate moderately stable ligand systems. These can be used as ligands to stabilize transition metal organometallics in their various oxidation states. By restricting the scope of this review to various phosphines and phosphinites, we have been able to provide a comprehensive summary of silylphosphines. Among, several phosphines described in the review the preeminent ones are $R_2Si\{(CH_2)_nPR'_2\}_2$ and $RSi\{(CH_2)_nPR'_2)\}_3$ which show interesting coordination behavior, their platinum metal derivatives also show good catalytic properties. The ligands with one or more Si–H bonds would be interesting as they can establish a direct metal–Si σ-bond by elimination of HCl or H_2 and also by hydrogen migration depending on the reaction conditions as seen in the reactions of biPSiH and triPSiH with platinum metals. In the reaction of $MeMn(CO)_5$ with $Me_2Si(CH_2PPh_2)_2$, the methyl group on manganese abstracts a proton from one of the silyl-methyl groups to establish a methylene bridge between Mn and Si atoms with the elimination of a molecule of methane as shown in Scheme 20 (complex **63**). The bis(phosphine) with P–N–Si–N–P framework reported by Woollin's group shows interesting reactivity. Triazasilatranes synthesized by Verkade's group are other examples of silylphosphines with rich coordination chemistry. The coordination behavior of silylalkylphosphines is comparable with those of carbon-bridged analogues. Surprisingly, the chemistry of silyl esters with Si–O–P bonds is not developed and the transition metal chemistry is sparse. The incorporation of a silyl moiety into the bis(phosphine) system was seen in the thermal reaction of $[MoH_4(dppe)_2]$ with $PhSiH_3$ which affords an unusual quadruply chelated complex **218** via *o*-C–H activation of phenyl groups present on the phosphorus centers of dppe ligands (Scheme 44). This reaction describes a new avenue to generate silicon-bridged phosphines at metal centers without breaking the M–P linkages. Overall, this review has demonstrated the versatility of various silylphosphines and their utility in catalysis. The highlights of these ligands are: (i) the organosilicon group solubilizes the ligands as well as their metal complexes, (ii) the organosilicon group provides an excellent NMR handle, (iii) most of the ligands with organosilicon groups are liquids and are volatile, (iv) the steric and electronic properties can be tuned readily at silicon center(s), (v) a variety of polyphosphines can be synthesized with a variety of heteroatoms as spacers along with organosilicon groups that enhance the flexibility of the ligand system, (vi) the organosilicon groups act as anchoring units to hold the phosphorus moieties when they are not bound directly. Platinum metal complexes of these compounds can be very good homogeneous catalysts for organic synthesis and also for co-polymerization.

The contents of this review and the above highlights are encouraging for the future use of this class of ligands in various facets of chemistry.

Copolymerization of ethylene and CO

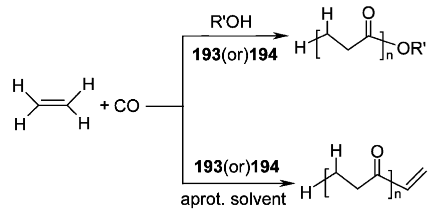

TON (mol/mol Pd) of **193** is 2100 whereas **194** is inactive (TON=0)

Scheme 50.

7. List of compounds[a] with ^{31}P-NMR data[b]

Compound number	Compound (yield)	^{31}P-NMR data	Reference
1*	$[Li\{PMe_2C(SiMe_3)_2\}(THF)]_2$ (88)	–	[33]
2*	$[Li\{\eta^2\text{-}C(PPh_2)_2(SiMe_3)\}(TMEDA)]$ (83)	22.61 ($J_{Li-P} = 48.6$)	[34]
3	$[(TMEDA)Li\{C(PMe_2)(SiMe_3)_2\}_2Li]$	–	[35]
4*	$[\{Li(TMEDA)(PMe_2)CH(SiMe_3)\}_2]$	–	[35]
5	$[Li\{C(PMe_2)(SiMe_3)_2\}(SiMe_4)_2]_2$	–	[33]
6	$[Li\{C_5H_5(SiMe_2)CH_2PPh_2\}]$ (94)	–	[65]
7	$[Li\{C_5H_5(SiMe_2)CH_2CH_2PPh_2\}]$ (88)	–	[64]
8*	$[Li\{P(CH(SiMe_3)_2)_2\}]_2$	-254 (sep, $J_{Li-P} = 80$)	[36]
9*	$[Mg(\eta^2\text{-trimpsi})\{SeSi(SiMe_3)_3\}_2]$ (73)	–	[37]
10*	$[TiBH_4\{\eta^2\text{-trimpsi}\}Cp^*]$ (55)	–	[38]
11*	$[Ti(CO)_4\{\eta^3\text{-trimpsi}\}]$ (21)	-10.8 (q, $J_{P-C} = 8.2$)	[39]
12*	$[Ti\{\eta^3\text{-trimpsi}\}(\eta^6\text{-}C_{10}H_8)]$ (40)		[40]
13	$[ZrCl_2\{(C_5H_4SiMe_2CH_2PPh_2)_2\}]$ (46)	–	[42]
14	$[ZrCl_2\{(C_5H_4SiMe_2(CH_2)_2PPh_2)_2\}]$ (34)	–	[42]
15	$[ZrCl(H)\{(C_5H_4SiMe_2(CH_2)_2PPh_2)_2\}]$ (90)	–	[42]
16	$[Zr(H)_2\{(C_5H_4SiMe_2(CH_2)_2PPh_2)_2\}]$ (55)	–	[42]
17	$[Zr((CH_2)_2R)Cl\{(C_5H_4SiMe_2(CH_2)_2PPh_2)_2\}]$ (75)	–	[42]
18	$[ZrCl_2\{C_5H_4SiMe_2(CH_2)_2PPh_2Co(CO)_3\}_2]$ (85)	–	[42]
19	$[VCl_3\{\eta^3\text{-trimpsi}\}\ (THF)]$ (80)	–	[45]
20*	$[V\{\eta^3\text{-trimpsi}\}\ (CO)_3H]$ (35)	14.20 (octet, $J_{PV} = 200$)	[45]
21	$[V\{\eta^3\text{-trimpsi}\}\ (CO)_3]^+$ (5)	–	[45]
22	$[Nb\{\eta^3\text{-trimpsi}\}(CO)_3I]$ (82)	-17.8 (b.s)	[44,45]
23*	$[Ta\{\eta^3\text{-trimpsi}\}(CO)_3I]$ (84)	-32.98 (b.s)	[44,45]
24*	$[Nb\{\eta^3\text{-trimpsi}\}(CO)_2(NO)]$ (88)	-20	[44,45]
25*	$[Ta(\eta^3\text{-trimpsi})(CO)_2NO]$ (90)	-33.2 (1P), -24.0 (2P)	[44,45]
26*	$[V\{\eta^3\text{-trimpsi}\}(CO)_2NO]$ (59)	-10 (octet, $J_{PV} = 130$, 1P), 5.0 (octet, $J_{PV} = 220$)	[45]
27*	$[Nb\{\eta^3\text{-trimpsi}\}(\eta^6\text{-}C_6H_5Me)]$ (65)	–	[46,47]
28	$[Nb(\eta^3\text{-trimpsi})(\eta^6\text{-}C_6H_5Me)H]$ (45)	1.1 (br.S)	[46,47]
29*	$[(CO)_5Cr{=}Si\{C_6H_4CH_2PPh_2\text{-}o\}_2]$ (34)	1.78	[48]
30	$[(CO)_4Cr{=}Si\{C_6H_4CH_2PPh_2\text{-}o\}_2]$	–	[48]
31	$[(CO)_3Cr{=}Si\{C_6H_4CH_2PPh_2\text{-}o\}_2]$ (80)	42.9	[48]
32*	$[CrMe_3\{\eta^3\text{-trimpsi}\}]$	–	[49]
33*	$[Cr^nBu_3\{\eta^3\text{-trimpsi}\}]$	–	[49]
34	$[Mo(CO)_4\{\eta^2\text{-}(Me_2Si(CH_2PPh_2)_2\}]$	43.3	[50]
35	$[Mo(CO)_3Br_2\{\eta^2\text{-}(Me_2Si(CH_2PPh_2)_2\}]$	34.7, 23.5	[50]
36*	$[Cr(CO)_4\{\eta^2\text{-}(^tBu_2Si(OPPh_2)_2\}]$		[28]
37*	$[Mo(CO)_4\{\eta^2\text{-}(^tBu_2Si(OPPh_2)_2\}]$		[28]
38	$[W(CO)_4\{\eta^2\text{-}(^tBu_2Si(OPPh_2)_2\}]$		[28]
39	$[Mo(CO)_4\{\eta^2\text{-}(Me_2Si(OP(OMe)_2)_2\}]$ (76)	148.8	[15]
40	$[Mo(CO)_4\{\eta^2\text{-}(Ph_2Si(OP(OMe)_2)_2\}]$ (77)	149.4	[15]
41	$[Mo(CO)_4\{\eta^2\text{-}(MePhSi(OP(OMe)_2)_2\}]$ (79)	148.8	[15]
42	$[Mo(CO)_4\{\eta^2\text{-}(Me(CH{=}CH_2)Si(OP(OMe)_2)_2\}]$	148.3	[15]
43	$[Mo(CO)_4\{\eta^2\text{-}(Me_2Si(OPPh_2)_2\}]$	128.39	[54]
44	$[Mo(CO)_4\{\eta^2\text{-}(MePhSi(OPPh_2)_2\}]$	130.50	[54]
45	$[Mo(CO)_4\{\eta^2\text{-}(MeEtSi(OPPh_2)_2\}]$ (87)	128.16	[54]
46	$[Mo(CO)_4\{\eta^2\text{-}(Me(CH_2Cl)Si(OPPh_2)_2\}]$ (42)	132.17	[54]
47*	$[Mo(CO)_4\{\eta^2\text{-}(MePhSi(OP(OMe)_2)_2\}]$	–	[51]

48*	$[Mo(CO)_4\{\eta^2\text{-}(Me_2Si(OP(OCH_2CMe_2CH_2O))\}]$	–	[55]
49*	$[Mo(CO)_4\{\eta^2\text{-}(Me^tBuSi\{OP(OCH_2C\text{-}Me_2CH_2O)\}_2\}]$	–	[55]
50*	$[Mo(CO)_4\{\eta^2\text{-}(Me^tBuSi(OPPh_2)_2\}]$	–	[55]
51*	$[Mo(CO)_4\{\eta^2\text{-}(Ph_2Si(OP(OMe)_2)_2\}]$	–	[51]
52	$[\{Mo(CO)_4\}_2\{\eta^4\text{-}(Si(OPPh_2)_4\}]$ (95)	–	[56]
53	$[Mo(CO)_4\{\eta^2\text{-}(Me_2Si(NHPPh_2)_2\}]$ (70)	–	[56]
54	$[Mo(CO)_4\{\eta^2\text{-}(MePhSi(NHPPh_2)_2\}]$ (88)	–	[56]
55	$[Mo(CO)_4\{\eta^2\text{-}(MeSi(OP(OMe)_2)_3\}]$	149.8 (S, 2P), 125.5 (S, 1P)	[30]
56*	$[Mo(CO)_3\{\eta^3\text{-}(MeSi(OP(OMe)_2)_3\}]$ (70)	153.5	[30]
57	$[Mo(CO)_3\{\eta^3\text{-}(PhSi(OP(OMe)_2)_3\}]$	153.7	[30]
58	$[Mo(CO)_3\{\eta^3\text{-}(CH{=}CH_2)Si(OP(OMe)_2)_3\}]$	153.5	[30]
59*	$[Mo(CO)_3\{\eta^3\text{-}(Ph_2SiPPh)_3\}]$ (52)		[57]
60	$[W\{\eta^3\text{-tmps}\}\ (\eta^6\text{-}C_6H_5Me)]$ (70)	-32.8 ($J_{PW} = 395$)	[58]
61	$[WH\{\eta^3\text{-tmps}\}(\eta^6\text{-}C_6H_5Me)][BF_4]$ (75)	-33.3 ($J_{PW} = 260$)	[58]
62	$[Mn(CO)_3Br\{\eta^2\text{-}Me_2Si(CH_2PPh_2)_2\}]$	35.8, 33.2, 13.2	[50]
63*	$[Mn(CO)_3Br\{\eta^3\text{-}MeSiCH_2(CH_2PPh_2)_2\}]$	–	[59]
64*	$[Mn(CO)_3Br\{\eta^2\text{-}Me_2Si(OP(OMe)_2)_2\}]$ (59)	149.3	[14]
65	$[Mn(CO)_3Br\{\eta^2\text{-}Ph_2Si(OP(OMe)_2)_2\}]$ (42)	149.9	[14]
66	$[Mn(CO)_3Br\{\eta^2\text{-}MePhSi(OP(OMe)_2)_2\}]$ (49)	149.3	[14]
67	$[Mn(CO)_3Br\{\eta^2\text{-}Me(CH{=}CH_2)Si(OP(OMe)_2)_2\}]$	149.4	[14]
68	$[Mn(CO)_3Br\{\eta^2\text{-}Me_2Si(OP(tolyl)_2)_2\}]$ (51)	137.7	[29]
69	$[Fe\{\eta^3\text{-tmps}\}(\eta^4\text{-}C_6H_6)]$ (68)	26.53 (s), 27.72 (s)	[61,60]
70	$[Fe\{\eta^3\text{-tmps}\}(CO)_2]$ (90)	–	[60]
71	$[Fe\{\eta^3\text{-tmps}\}(\eta^2\text{-}PhCCPh)]$ (77)	–	[61,60]
72	$[Fe\{\eta^3\text{-tmps}\}(\eta^2\text{-}MeCCEt)]$ (58)	37.78	[60]
73	$[Fe\{\eta^3\text{-tmps}\}(\eta^2\text{-}EtCCEt)]$ (50)	32.49	[60]
74	$[Fe\{\eta^3\text{-tmps}\}(\eta^2\text{-}SiMe_3CCSiMe_3)]$ (50)	33.81	[60]
75*	$[Fe_2\{\eta^3\text{-tmps}\}_2\ (\mu\text{-}H)_2(\mu\text{-}C{=}CH_2)]$ (40)	34.39 (4P, vt, $J_{PP} = 7$), 12, 14 (2P)	[61,60]
76	$[Fe\{\eta^3\text{-tmps}\}(\eta^4\text{-}C_6H_8)]$ (72)	28.56	[60]
77	$[FeH\{\eta^2\text{-tmps}\}(\eta^5\text{-}C_5H_5)]$ (30)	42.26 (S, 2P), -59.43 (S, 1P)	[60]
78	$[Fe\{\eta^3\text{-tmps}\}(\eta^4\text{-}C_6H_5(CH_2)_2Ph)]$ (95)	29.28 (S), 26.71 (d, 1P), 25.38 (d, 1P) ($J_{PP} = 54$)	[60]
79	$[Fe\{\eta^3\text{-tmps}\}(\eta^5\text{-}C_6H_6(CH_2)_2Ph)]PF_6$ (94)	–	[60]
80	$[FeCl_2\{\eta^3\text{-tmps}\}]$	39.3(S)	[61]
81	$[Fe_2\{\eta^3\text{-tmps}\}_2\ (\mu\text{-}Cl)_3]Cl$ (95)	–	[60]
82	$[Fe_2\{\eta^3\text{-tmps}\}_2\ (\mu\text{-}Cl)_3]BPh_4$ (80)	–	[60]
83	$[Fe\{\eta^3\text{-tmps}\}(\eta^4\text{-}C_4H_6)]$ (90)	31.42 (t), 30.05 (d) ($J_{PP} = 14$)	[60]
84	$[Fe\{\eta^3\text{-tmps}\}(\eta^5\text{-}C_5H_5)]PF_6$ (60)	–	[60]
85	$[Fe\{\eta^3\text{-tmps}\}(\eta^2\text{-dmpe})]$ (72)	55.6 (q, $J = 30$, dmpe), 13.0 (t, tmps)	[63]
86	$[FeH\{\eta^3\text{-tmps}\}(\eta^2\text{-dmpe})]PF_6$ (64)	57.7 (m, 2P, dmpe), 22.8 (m, 2P), 11.2 (m, 1P)	[63]
87	$[Fe\{C_5H_4SiMe_2CH_2PPh_2\}_2]$ (85)	-30.4	[41,65]
88	$[Fe(C_5H_4SiMe_2(CH_2)_2PPh_2)_2]$ (76)	-9.1	[64]
89	$[Fe(C_5H_4SiMe_2CH_2PPh_2)_2]NiCl_2$ (75)	-6.4	[41,65]
90	$[Fe(C_5H_4SiMe_2CH_2PPh_2)_2]NiBr_2$ (36)	2.4	[41,65]
91	$[Fe(C_5H_4SiMe_2(CH_2)_2PPh_2)_2]NiCl_2$ (64)	-27.3	[64]
92	$[Fe\{C_5H_4SiMe_2(CH_2)_2PPh_2\}_2NiBr_2]_2$ (86)	15.6	[64]
93	$[Fe\{C_5H_4SiMe_2(CH_2)_2PPh_2\}_2NiCl_2]_2$	-5.5	[65]
94	$[Fe\{C_5H_4SiMe_2(CH_2)_2PPh_2\}_2NiBr_2]_2$ (36)	2.4	[65]
95	$[Fe\{C_5H_4SiMe_2(CH_2)_2PPh_2\}_2Co_2(CO)_8]_2$ (74)	66.3	[64]
96	$[Fe\{C_5H_4SiMe_2CH_2PPh_2\}_2Mo(CO)_4]_2$ (30)	12.3, 14.4, 24.9	
97	$[Fe\{C_5H_4SiMe_2CH_2PPh_2\}_2Mo(CO)_4]_2$ (30)	12.3, 14.4, 24.9	[65]
98	$[Fe(C_5H_4SiMe_2CH_2PPh_2\}_2Mo(CO)_4]_2$ (30)	12.3, 14.4, 24.9	[65]
99	$[Fe(C_5H_4SiMe_2CH_2PPh_2\}_2Mn(CO)_3Br]_2$ (40)	39.2, 39.6, 40.3, 40.5	[65]
100	$[Fe(C_5H_4SiMe_2CH_2PPh_2\}_2Mn(CO)_3Br]_2$ (40)	39.2, 39.6, 40.3, 40.5	[65]

101	$[Fe\{C_5H_4SiMe_2CH_2PPh_2\}_2Co_2(CO)_6]$ (39)	46.3	[65]
102	$[Fe(C_5H_4SiMe_2CH_2PPh_2(O))_2]$	22	[65]
103	$[Fe(C_5H_4SiMe_2CH_2PPh_2Co(CO)_3)_2](PPN)_2$	–	[65]
104	$[RuCl_2\{\eta^3\text{-tmps}\}(PMe_3)]$ (88)	20.6 (2P), 3.71 (PMe_3), −14.4 (1P) ($J_{PP} = -36.2, -28.0, 319.2$)	[66]
105	$[RuH\{\eta^3\text{-tmps}\}(PMe_3)(\eta^1\text{-}C_6H_5)]$ (81)	6.57(1P), −1.89(1P),-3.54(1P), −11.18 (1P), ($J_{PP} = -23, 265.3, -26.8, -26.5, -21.3, -27.4$)	[66]
106	$[RuH\{\eta^3\text{-tmps}\}\ (\eta^2\text{-}CH_2PMe_2)]$ (63)	14.42 (1P), 8.69 (1P), −3.30 (1P), −31.21 (1P), ($J_{PP} = -11.1, -26.9, 192.6, -14.6, -27, -35.5$)	[66]
107	$[RuH\{\eta^3\text{-tmps}\}(PMe_3)(\eta^2\text{-}CH_2CMe_2CD_2)]$ (58)	–	[69]
108	$[RuH\{\eta^3\text{-tmps}\}(PMe_3)(\eta^2\text{-}CH_2SiMe_2CH_2)]$ (78)	1.70 (dt, $J_{PP} = 299, 30$), −6.76 (dt, $J = 299, 30$), −12.2 (dd, $J = 30, 30$)	[69]
109	$[RuH\{\eta^3\text{-tmps}\}(PMe_3)(\eta^2\text{-}CH_2CMe_2CH_2)]$ (71)	1.13 (PMe_2), −4.20 (PMe_3) (dt, $J = 315, 29$), −12.2 (dd, $J = 28, 29$)	[69,67]
110	*Endo*-$[RuMe\{\eta^3\text{-tmps}\}(\ (\eta^3\text{-}CH_2CMeCH_2)]$ (93)	8.91 (d, $J = 23$), −7.73 (t, $J = 23$)	[69,67]
111	*Exo*-$[RuMe\{\eta^3\text{-tmps}\}(\eta^3\text{-}CH_2CmeCH_2)]$ (93)	8.23 (d, $J = 27$), −7.10 (t, $J = 23$)	[69,67]
112	$[RuMe_2\{\eta^3\text{-tmps}\}(PMe_3)]$ (63)	7.50 (dt, $J = 322, 28$), 0.96 (321, 27), −5.93 (dd, $J = 28, 27$)	[69]
113	$[RuCl\{\eta^3\text{-tmps}\}(Me)(PMe_3)]$	22.9 (dd, $J = 24, 31, 40$), 5.8 (ddd $J = 25, 44, 324$), −7.3 (ddd, $J = 28, 30, 32$), −9.8 (ddd, $J = 23, 23, 23$)	[69]
114	$[RuH\{\eta^3\text{-tmps}\}(PMe_3)(\eta^4\text{-}(CH_2)_3C)]$ (29)	7.99	[69]
115	$[RuCl\{\eta^3\text{-tmps}\}(PMe_3)(H)]$ (95)	25.07 (dt, $J_{PP} = 35, 25$), 6.51 (ddd, $J_{PP} = 277, 35, 25$), 5.07 (dt, $J_{PP} = 277, 25$)	[70]
116	$[RuH_2\{\eta^3\text{-tmps}\}(PMe_3)]$ (91)	9.75 (dt, $J_{PP} = 244, 27$), 0.64 (dt), −1.50 (t, $J_{PP} = 27$)	[70]
117	$[RuH\{\eta^3\text{-tmps}\}(PMe_3))(NH_3)]BPh_4$ (84)	24.68 (dt, $J_{PP} = 36, 25$), 9.29 (ddd, $J_{PP} = 248, 36, 25$), −2.11 (ddd, $J_{PP} = 249, 36, 25$), −4.99 (q, $J_{PP} = 25$)	[70]
118	$[RuH\{(PMe_2CH_2)_2SiMe(\eta^2\text{-}CHPMe_2)\}\text{–}(PMe_3)]$ (75)	14.12 (ddd, $J_{PP} = 175, 27, 7$), 11.37 (dt, $J_{PP} = 175, 27$), 6.55 (td, $J_{PP} = 27, 7$), −1.53 (q, $J_{PP} = 27$)	[70]
119	$[RuCl\{(PMe_2CH_2)_2SiMe(\eta^2\text{-}CHPMe_2)\}\text{–}(PMe_3)]$ (84)	33.4 (q, $J_{PP} = 35$), 15.08 (dd, $J_{PP} = 233, 35$), 7.27 (dt, $J_{PP} = 233, 35$), 4.28 (t, $J_{PP} = 35$)	[70]
120	$[Ru\{(PMe_2CH_2)_2SiMe(\eta^2\text{-}CHPMe_2)\}(OTf)(PMe_3)]$ (87)	42.16 (q, $J_{PP} = 35$), 10.15 (dd, $J_{PP} = 212, 35$), 3.10 (dt, $J_{PP} = 212, 35$), −1.54 (t, $J_{PP} = 35$)	[70]
121	$[RuMe\{(PMe_2CH_2)_2SiMe(\eta^2\text{-}CHPMe_2)\}\text{–}(PMe_3)]$ (63)	11.84 (dd, $J_{PP} = 214, 27$), 3.55 (t, $J_{PP} = 28$), 2.17 (dt, $J_{PP} = 214, 27$), −1.44 (q, $J_{PP} = 27$)	[70]
122	$[RuH\{\eta^3\text{-tmps}\}(PMe_3)(Me)]$ (80)	9.27 (dt, $J_{PP} = 285, 27$), 1.67 (dt), −1.53 (q, $J_{PP} = 27$), −5.23 (q)	[70]
123	$[RuH\{\eta^3\text{-tmps}\}(PMe_3)(\eta^2\text{-}CH_2PMe_2)]$ (79)	14.49 (ddd, $J_{PP} = 193, 28, 11$), 8.65 (td, $J_{PP} = 28, 11$), −3.28 (q, $J_{PP} = 28$), −31.20 (ddd, $J_{PP} = 193, 37, 11$)	[70]
124	$[RuH\{\eta^3\text{-tmps}\}(PMe_3)(OTol)]$ (81)	24.07 (q, $J_{PP} = 30$), 10.58 (dt, $J_{PP} = 289, 30$), 0.10 (dt, $J_{PP} = 289, 30$), −5.75 (q, $J_{PP} = 30$)	[70]
125*	*Syn*-$[RuCl\{\eta^3\text{-}MeSi((CH_2)_3PPh_2)_2\}(CO)]$	17.6	[71]
126	*Anti*-$[RuCl\{\eta^3\text{-}MeSi((CH_2)_3PPh_2)_2\}(CO)]$	26.4	[71]
127*	$[RuCl\{\eta^3\text{-}MeSi((CH_2)_3PPh_2)_2\}(CO)_2]$	14.7	[71]

128	*Syn*-$[RuH\{\eta^3\text{-}MeSi((CH_2)_3PPh_2)_2\}(CO)_2]$		[73]
129	*Anti*-$[RuH\{\eta^3\text{-}MeSi((CH_2)_3PPh_2)_2\}(CO)_2]$	32.9	[73]
130	*Trans*-$[RuCl\{\eta^3\text{-}MeSi((CH_2)_3PPh_2)_2\}(CO)_2]$	14.7	[73]
131	*Cis*-$[RuCl\{\eta^3\text{-}MeSi((CH_2)_3PPh_2)_2\}(CO)_2]$	13.9	[73]
132	$[RuH_2\{\eta^3\text{-}MeSi((CH_2)_3PPh_2)_2\}(CO)]$		[73]
133	$[RuH\{\eta^3\text{-}MeSiO((CH_2)_3PPh_2)_2\}(CO)_2]$	43.6	[74]
134	$[RuH\{\eta^3\text{-}MeOSiO((CH_2)_3PPh_2)_2\}(CO)_2]$ (80)	33.8	[74]
135	$[RuH\{\eta^3\text{-}MeSiO((CH_2)_3PPh_2)_2\}(^{13}CO)_2]$	33.9	[74]
136*	$[RuH\{\eta^3\text{-}MeSiO((CH_2)_3PPh_2)_2\}(CO)(P(OMe)_3)]$	135.7 (t, $J_{PP} = 24.4$), 40 (d)	[74]
137*	$[RuH\{\eta^3\text{-}MeOSiO((CH_2)_3PPh_2)_2\}(CO)\text{–}(P(OMe)_3)]$ (90)	135.9 (t, $J_{PP} = 25$), 41.6 (d)	[74]
138	$[RuH\{\eta^3\text{-}MeSi((CH_2)_2PPh_2)_2\}(CO)_2]$ (15)	–	[75]
138*	$[RuH\{\eta^3\text{-}MeSi((CH_2)_3PPh_2)_2\}(CO)_2]$ (8)	–	[74]
140	$[Ru(CO)_3]_3\{\eta^3\text{-}MeSi(PEt_2)_3\}]$ (14)	−26.8	[79]
141	$[\{Ru(CO)_3\}_3\{\eta^3\text{-}MeSi(PPr_2)_3\}]$ (7)	−33.5	[79]
142*	$[\{Ru(CO)_3\}_3\{\eta^3\text{-}MeSi(PBu_2)_3\}]$ (16)	33.7	[79,76]
143	$[Ru(\eta^3\text{-}C_4H_7)_2\{\eta^2\text{-}Me_2Si(CH_2PPhNp)_2\}]$ (78)	−35.74	[23]
144	$[Ru(\eta^3\text{-}C_4H_7)_2\{\eta^2\text{-}Me_2Si(CH_2PPho\text{-}An)_2\}]$		
145	$[RuCl_2(PPh_3)\{\eta^2\text{-}Me_2Si(CH_2PPhNp)_2\}]$ (89)	39.7, 35.2, 103.8 ($^2J_{AB} = 303.5$, $^2J_{AX} = 28.7$, $^2J_{BX} = 39.6$)	[23]
146	$[CoCl_2\{\eta^2\text{-}Me_2Si(CH_2PPh_2)_2\}]$ (60)	–	[78]
147*	$[CoBr_2\{\eta^2\text{-}Me_2Si(CH_2PPh_2)_2\}]$ (60)	–	[78]
148	$[Co(NO_3)_2\{\eta^2\text{-}Me_2Si(CH_2PPh_2)_2\}]$ (60)	–	[78]
149	$[Co(ClO_4)_2\{\eta^2\text{-}Me_2Si(CH_2PPh_2)_2\}]$ (60)	–	[78]
150	$[Co(SCN)_2\{\eta^2\text{-}Me_2Si(CH_2PPh_2)_2\}]$ (60)	–	[78]
151	$[CoI_2\{\eta^2\text{-}Me_2Si(CH_2PPh_2)_2\}]$ (60)	–	[78]
152	$[Co_4(CO)_9\{\eta^3\text{-}MeSi(PEt_2)_3\}]$ (31)	-1.5	[79]
153	$[Co_4(CO)_9\{\eta^3\text{-}MeSi(PPr_2)_3\}]$ (55)	-7.7	[79]
154	$[Co_4(CO)_9\{\eta^3\text{-}MeSi(PBu_2)_3\}]$ (50)	−7.25	[79]
155	$[Rh_4(CO)_9\{\eta^3\text{-}MeSi(PEt_2)_3\}]$ (51)	−30.3 (dm) ($J_{Rh\text{–}P} = 106$)	[79]
156	$[Ir_4(CO)_9\{\eta^3\text{-}MeSi(PEt_2)_3\}]$ (5)	−45.3	[79]
157	$[Rh_6(CO)_{13}\{\eta^3\text{-}MeSi(PBu_2)_3\}]$ (5)	−21.8 (dm) ($J_{Rh\text{–}P} = 110$)	[79]
158	$[Rh(NBD)\{\eta^2\text{-}Me_2Si(CH_2PPhNp)_2\}BF_4]$ (81)	18.0 (d, $J_{Rh\text{–}P} = 160$)	[23]
159	$[Rh(COD)\{\eta^2\text{-}Me_2Si(CH_2PPhNp)_2\}BF_4]$ (92)	17.6(d,$J_{Rh\text{–}P} = 144.7$)	[23]
160	$[Rh(NBD)\ \{\eta^3\text{-}MeSi(CH_2PPh_2)_3\}]$Otf (98)	7.3 (d, $J_{Rh\text{–}P} = 117.9$)	[31]
161	$[Rh(NBD)\ \{\eta^3\text{-}MeSn(CH_2PPh_2)_3\}]$Otf (90)	13.7(d,$J_{Rh\text{–}P} = 119.6$)	[31]
162	$[Rh\ (CO)_2\{\eta^3\text{-}MeSn(CH_2PPh_2)_3\}]BPh_4$ (95)	5.5 (d, $J_{Rh\text{–}P} = 103$)	[31]
163	$[Rh\ (CO)_2\{\eta^3\text{-}MeSn(CH_2PPh_2)_3\}]$Otf (85)	6.2 (d, $J_{Rh\text{–}P} = 103$)	[31]
164	$[RhH\{\eta^4\text{-}Si(CH_2)_2PPh_2)_3\}Cl]$	−100.1 (dd) ($J_{Rh\text{–}P} = 114.9$), −110.5 (dt) ($J_{PP} = 19.3$, $J_{Rh\text{–}P} = 97.5$)	[81]
165	$[RhH\{\eta^4\text{-}Si(CH_2)_2PPh_2)_3\}(SnCl_3)]$	−83.9(dd)($J_{Rh\text{–}P} = 107.1$, $J_{PP} = 15.3$, $J_{Sn\text{–}P} = 132$), −94.9 (dt) ($J_{Rh\text{–}P} = 91.4$, $J_{Sn\text{–}P} = 323$)	[81]
166*	$[Rh\{\eta^4\text{-}Si(CH_2)_2PPh_2)_3\}(CO)]$	−79.8 (d) ($J_{Rh\text{–}P} = 155.1$)	[81]
167*	$[IrH\{\eta^3\text{-}MeSi(CH_2)_3PPh_2)_2\}Cl\}]$ (95)	10.2	[75]
168, **169**	$[IrCl\{\eta^3\text{-}MeSi(CH_2)_3PPh_2)_2\}(H)(CO)]$ (66)	−16.1, −11	[75]
170, **171***	$[IrH\{\eta^3\text{-}MeSi((CH_2)_3PPh_2)_2\}(CO)(SnCl_3)]$ (98)	−22.5 ($^2J_{p\text{-}Sn} = 126$) −14.3 ($^2J_{P\text{-}Sn} = 247$)	[75]
172–**175**	$[Ir\{\eta^3\text{-}MeSi((CH_2)_3PPh_2)_2\}(H)_2(CO)]$ (52)	−8.9, −5.5	[75]
176	$[IrCl(H)\{\eta^4\text{-}Si(CH_2C_6H_4PPh_2\text{-}o)_3\}]$ (91)	−5.3, −11.4	[16]
177*	$[Ni\{\eta^2\text{-}Me_2Si(CH_2PPh_2)_2\}(NO_3)_2]$	–	[84]
178	$[NiCl_2\{\eta^2\text{-}Me_2Si(CH_2PPh_2)_2\}]$	–	[50]
179	$[PdCl_2\{\eta^2\text{-}Me_2Si(CH_2PPh_2)_2\}]$	23.2	[50]
180	$[Pd(\eta^2\text{-}C_6H_4CH(Me)NMe_2\text{-}o)\{\eta^2\text{-}Me_2\text{-}Si(CH_2P(Np)Ph)_2\}]PF_6$	33.21 (d), 11.82 (d) ($J_{PP} = 45$)	[23]
181	$[Pt\{\eta^3\text{-}MeSi((CH_2)_2PPh_2)_2\}Cl]$ (84)	–	[75]

182	$[Pt\{\eta^3\text{-}MeSi((CH_2)_2PCy_2)_2\}Cl]$ (84)	63.3 ($J_{PPt} = 2981$)	[75]
183	$[Pt\{\eta^3\text{-}PhSi((CH_2)_2PCy_2)_2\}Cl]$ (35)	61.9 ($J_{PPt} = 2903$)	[75]
184*	$[Pt\{\eta^3\text{-}MeSi((CH_2)_3PPh_2)_2\}Cl]$ (73)	8.6 ($J_{PPt} = 2825$)	[75]
185	$[Pt(\eta^3\text{-}MeSi((CH_2)_3PCy_2)_2\}Cl]$ (76)	13.0 ($J_{PPt} = 2714$)	[75]
186	$[Pt\{\eta^3\text{-}PhSi((CH_2)_3PPh_2)_2\}Cl]$ (72)	8.2 ($J_{PPt} = 2729$)	[75]
187	$[Pt\{\eta^3\text{-}PhSi((CH_2)_2PCy_2)((CH_2)_2PPh_2)\}Cl]$ (75)	44.9($J_{PPt} = 2952$) 62.5 ($J_{PPt} = 2855$)	[75]
188, 189	$[PtH\{\eta^2\text{-}MeClSi((CH_2)_3PPh_2)_2\}Cl]$	23.4 ($J_{PPt} = 2964$) 23.0 ($J_{PPt} = 2959$)	[75]
190	$[Pt\{\eta^3\text{-}MeSi(CH_2C_6H_4PPh_2\text{-}o)_2\}Cl]$ (27)	22.3 ($J_{Pt-P} = 2908$)	[16]
191*	$[Pt\{\eta^2\text{-}Ph_2Si(OPPh_2)_2\}Cl_2]$	73.9 ($J_{Pt-P} = 4053$)	[85]
192	$[Pt\{\eta^2\text{-}Me_3Si(OPPh_2)_2\}(PEt_3)Cl]$	126.5($J_{Pt-P} = 2151$), 82.2 ($J_{Pt-P} = 3960$), 58.4 ($J_{Pt-P} = 2766$) $J_{PP} = 19, 21, 412$)	[86]
193	$[Pd\{\eta^2\text{-}Me_2Si(OPPh_2)_2\}(Me)Cl]$	114.5 (d), 99.8 (d) ($J_{PP} = 34.2$)	[87]
194	$[Pd\{\eta^2\text{-}Me_2Si(C_6H_4OPPh_2\text{-}m)_2\}(Me)Cl]$	116.1	[87]
195	$[Pd\{\eta^2\text{-}Me_2Si(OPPh_2)_2\}(Me)(MeCN)]$		[87]
196	$[Pd\{\eta^2\text{-}Me_2Si(C_6H_4OPPh_2\text{-}m)_2\}(Me)(MeCN)]$		[87]
197	$[CuBr\{Me_2Si(CH_2PPh_2)(\eta^2\text{-}CH{=}CH_2)\}]_2$ (45)	−14.98	[88]
198	$[ZnCl_2\{\eta^2\text{-}Me_2Si(CH_2PPh_2)_2\}]$	−24.8	[50]
199*	$[CdCl_2\{\eta^2\text{-}Me_2Si(CH_2PPh_2)_2\}]$ (72)	−15.5 ($J_{PCd} = 1248.5$)	[89]
200	$[CdBr_2\{\eta^2\text{-}Me_2Si(CH_2PPh_2)_2\}]$ (68)	−18.3 ($J_{PCd} = 1248.6$)	[89]
201	$[Cd_2I_2\{\eta^2\text{-}Me_2Si(CH_2PPh_2)_2\}]$ (65)	−25.0 ($J_{PCd} = 1154.6$)	[89]
202	$[Cd(NO_3)\{\eta^2\text{-}Me_2Si(CH_2PPh_2)_2\}]$ (80)	−8.6 ($J_{PCd} = 974.8$)	[89]
203	$[Cd(ClO_4)_2\{\eta^2\text{-}Me_2Si(CH_2PPh_2)_2\}]$	−8.6 ($J_{PCd} = 1756.4$)	[89]
204	$[Cd(SCN)_2\{\eta^2\text{-}Me_2Si(CH_2PPh_2)_2\}]$	−10.7	[89]
205	$[Cd\{\eta^2\text{-}Me_2Si(CH_2PPh_2)_2\}_2]$ $(ClO_4)_2$ (70)	−5.4 ($J_{PCd} = 1111.7$)	[89]
206	$[HgCl_2\{\eta^2\text{-}Me_2Si(CH_2PPh_2)_2\}]$ (75)	17.5 ($J_{PHg} = 3684$)	[90]
207	$[HgBr_2\{\eta^2\text{-}Me_2Si(CH_2PPh_2)_2\}]$ (75)	7.6 ($J_{PHg} = 3199$)	[90]
208	$[HgI_2\{\eta^2\text{-}Me_2Si(CH_2PPh_2)_2\}]$ (75)	−7.5 ($J_{PHg} = 2355$)	[90]
209	$[Hg(SCN)_2\{\eta^2\text{-}Me_2Si(CH_2PPh_2)_2\}]$ (73)	19.5 ($J_{PHg} = 3010$)	[90]
210	$[Hg_2Cl_4\{Me_2Si(CH_2PPh_2)_2\}]$ (76)	26.4 ($J_{PHg} = 7653$)	[90]
211	$[HgBr_2\{\eta^2\text{-}Me_2Si(OPPh_2)_2\}]$ (98)	–	[27]
212	$[PdCl_2\{Me_2Si(N(C_5H_4N\text{-}2)PPh_2)_2\}]$	64.44	[24]
213	$[PtCl_2\{Me_2Si(N(C_5H_4N\text{-}2)PPh_2\}_2]$	42.3 ($^1J_{PPt} = 3902$)	[24]
214*	$[Pt\{(NC_5H_4)NHPPh_2\}_2]$	51.4 ($^1J_{PPt} = 3576$)	[24]
215*	$[PtMe_2\{Me_2Si(N(C_5H_4N\text{-}2)PPh_2)_2\}]$	63.9 ($^1J_{PPt} = 1986$)	[24]
216	$[Me_2Si(N(C_5H_4N\text{-}2)PPh_2(Se))_2]$	47.6 ($^1J_{P-Se} = 778$)	[24]
217	$[(C_5H_4N\text{-}2)N(PPh_2)_2]$	59.9	[24]
218	$[Mo(H)_3\{\eta^5\text{-}Si(Ph)(C_6H_4PPh(CH_2)_2PPh_2)_2\}]$		[95]
219	$[Mo(H)_3\{\eta^5\text{-}Ge(Ph)(C_6H_4PPh(CH_2)_2PPh_2)_2\}]$		[95]
220*	$[Mo(H)(\eta^2\text{-}O_2)\{\eta^5\text{-}Si(Ph)(C_6H_4PPh{-}(CH_2)_2PPh_2)_2\}]$		[97]
221	$[Mo(H)_2(SiPhH)\{\eta^5\text{-}Si(Ph)(C_6H_4PPh{-}(CH_2)_2PPh_2)_2\}]$		[95]
222	$[Mo(H)_2(OCOH)\{\eta^5\text{-}Si(Ph)(C_6H_4PPh{-}(CH_2)_2PPh_2)_2\}]$ (82)		[96]
223*	$[Mo(H)_2(OCOMe)\{\eta^5\text{-}Si(Ph)(C_6H_4PPh{-}(CH_2)_2PPh_2)_2\}]$ (90)	87.7, 59.1 (d, $J_{PP} = 122$)	[96]
224	$[Mo(H)_2(OCOPh)\{\eta^5\text{-}Si(Ph)(C_6H_4PPh{-}(CH_2)_2PPh_2)_2\}]$		[96]
225	$[Mo(H)_2(OCOH)\{\eta^5\text{-}Ge(Ph)(C_6H_4PPh{-}(CH_2)_2PPh_2)_2\}]$		[96]
226	$[Mo(H)_2(OCOMe)\{\eta^5\text{-}Ge(Ph)(C_6H_4PPh{-}(CH_2)_2PPh_2)_2\}]$		[96]
227	$[Mo(H)_2(OCOPh)\{\eta^5\text{-}Ge(Ph)(C_6H_4PPh{-}(CH_2)_2PPh_2)_2\}]$		[96]
228*	$[Mo(H)_2\{\eta^2\text{-}OCH(Me)CH_2CH(Me)O\}{-}\{\eta^5\text{-}Si(Ph)(C_6H_4PPh(CH_2)_2PPh_2)_2\}]$ (54)	102.7 (m), 70.4 (m), −5.4 (m)	[98]

229	$[Mo(H)_2\{\eta^2\text{-}OCH(Me)CH_2CH(Me)O\}\text{–}\{\eta^5\text{-}Si(C_6H_4Me\text{-}o)(C_6H_4PPh(CH_2)_2PPh_2)_2\}]$ (51)	99.9 (m), 73.4 (m), 65.6 (m), −4.9(m)	[98]
230	$[Mo(H)_2(\eta^1\text{-}OC(OEt)CHC(O)(OEt))\text{–}\{\eta^5\text{-}Si(Ph)(C_6H_4PPh(CH_2)_2PPh_2)_2\}]$ (55)	104.1 (dd) ($J_{PP} = 61, 20$), 86.3 (dd) ($J_{PP} = 144, 12$), 57.3 (dd) $J_{PP} = 61, 20$) 48.8 (dd) ($J_{PP} = 149, 17$)	[98]
231	$[Mo(H)_2\{\eta^1\text{-}OC(O^iPr)CHC(O)(O^iPr)\}\text{–}\{\eta^5\text{-}Si(Ph)(C_6H_4PPh(CH_2)_2PPh_2)_2\}]$ (41)	103.7 (dd, $J_{PP} = 60, 12$), 85.7 ($J_{PP} = 150, 12$), 57.3 ($J_{PP} = 62, 18$), 48.7 (dd, $J_{PP} = 149, 17$)	[98]
232	$[Mo(H)_2\{\eta^1\text{-}OC(O^nPr)CHC(O)(O^nPr)\}\text{–}\{\eta^5\text{-}Si(Ph)(C_6H_4PPh(CH_2)_2PPh_2)_2\}]$ (36)	103.8 (dd, $J_{PP} = 60, 12$), 86.3 (dd, $J_{PP} = 147, 12$), 57.1 (dd, $J_{pp} = 60, 20$), 48.9 ($J_{PP} = 148, 20$)	[98]
233	$[Mo(H)_2\{\eta^1\text{-}OC(OCH_2C_6H_5)CHC(O)\text{–}(OCH_2C_6H_5)\}\{\eta^5\text{-}Si(Ph)(C_6H_4PPh\text{–}(CH_2)_2PPh_2)_2\}]$ (23)	103.8 (dd, $J_{PP} = 61, 12$), 87.7 (dd, $J_{PP} = 144, 12$), 57.1 (dd, $J_{PP} = 61, 20$), 48.7 ($J_{PP} = 148, 17$)	[98]

[a] Complexes with crystal structures are denoted by [*].

[b] Chemical shift (δ) is in ppm and J is in Hz, ^{31}P-NMR data are not available for all the compounds; d, doublet; dm, doublet of multiplets; t, triplet; q, quintet; m, multiplet; sep, septet.

Acknowledgements

This work is part of a research plan (M.S.B, 01(1701)/01/EMR-II) supported by CSIR, New Delhi, India. P.P.G. and P.C. thank the Department of Science and Technology, New Delhi and Indian Institute of Technology, Bombay for fellowships.

References

[1] W. Levason, C.A. McAuliffe, Adv. Inorg. Chem. Radiochem. 14 (1972) 173.
[2] R.J. Puddephatt, Chem. Soc. Rev. 12 (1983) 99.
[3] B. Chaudret, B. Delavaux, R. Poilblanc, Coord. Chem. Rev. 86 (1988) 191.
[4] M.S. Balakrishna, V.S.R. Reddy, S.S. Krishnamurthy, J.C.T.R. Burckette St. Laurent, J.F. Nixon, Coord. Chem. Rev. 129 (1994) 1 (and references cited therein).
[5] J.D. Woollins, T.Q. Ly, Coord. Chem. Rev. 176 (1998) 451.
[6] K.V. Katti, V.S.R. Reddy, R.P. Singh, Chem. Soc. Rev. (1995) 97.
[7] T.Q. Ly, A.M.Z. Slawin, J.D. Woollins, Angew. Chem. Int. Ed. Engl. 37 (1998) 2501.
[8] M.S. Balakrishna, R.M. Abhyankar, J.T. Mague, J. Chem. Soc. Dalton Trans. (1999) 1407.
[9] M.S. Balakrishna, R. Klein, S. Uhlenbrock, A.A. Pinkerton, R.G. Cavell, Inorg. Chem. 32 (1993) 5676.
[10] M.S. Balakrishna, B.D. Santarsiero, R.G. Cavell, Inorg. Chem. 33 (1994) 3079.
[11] M.S. Balakrishna, S. Teipel, A.A. Pinkerton, R.G. Cavell, Inorg. Chem. 40 (2001) 1802.
[12] M. Okazaki, S. Ohshitanai, M. Iwata, H. Tobita, H. Ogino, Coord. Chem. Rev. 226 (2002) 167.
[13] K. Issleib, B. Walther, Angew. Chem. Int. Ed. Engl. 6 (1967) 88.
[14] T.P. Kee, M.T. Patel, Polyhedron 11 (1992) 135.
[15] V. Sum, M.T. Patel, T.P. Kee, M. Thornton-Pett, Polyhedron 11 (1992) 1743.
[16] R.A. Gossage, G.D. McLennan, S.R. Stobart, Inorg. Chem. 35 (1996) 1729.
[17] M. Kranenburg, Y.E.M. van der Burgt, P.C.J. Kamer, P.W.N.M. van Leeuwen, K. Goubitz, J. Fraanje, Organometallics 14 (1995) 3081.
[18] M. Mirza-Aghayan, R. Boukherroub, G. Oba, G. Manuel, M. Koenig, J. Organomet. Chem. 564 (1998) 61.
[19] G. Oba, S. Phok, G. Manuel, M. Koenig, Tetrahedron 56 (2000) 121.
[20] L.F. Joslin, R.S. Stobart, Inorg. Chem. 32 (1993) 2221.
[21] E.C. Alyea, K.J. Fisher, R.P. Shakya, A.E. Vougioukas, Synth. React. Inorg. Met. -Org. Chem. 18 (1988) 163.
[22] K. Hassler, S. Seidl, Monatshefte fur Chemie 119 (1988) 1241.
[23] M.R. Stoop, A. Mezzetti, Organometallics 17 (1998) 668.
[24] S.M. Aucott, M.L. Clarke, A.M.Z. Slawin, J.D. Woollins, J. Chem. Soc. Dalton Trans. (2001) 972.
[25] X. Zhou, S.R. Stobart, R.A. Gossage, Inorg. Chem. 36 (1997) 3745.
[26] K. Hassler, U. Katzenbeisser, J. Organomet. Chem. 399 (1990) C18.
[27] K. Issleib, B. Walther, J. Organomet. Chem. 22 (1970) 375.
[28] H. Voelker, S. Freitag, U. Pieper, H.W. Roesky, Z. Anorg. Allg. Chem. 621 (1995) 694.
[29] K.M. Cooke, T.P. Kee, A.L. Langton, M. Thornton-Pett, J. Organomet. Chem. 419 (1991) 171.
[30] N. Greene, H. Taylor, T.P. Kee, M. Thornton-Pett, J. Chem. Soc. Dalton Trans. (1993) 821.
[31] S. Herold, A. Mezzetti, L.M. Venanzi, A. Albinati, F. Lianza, T. Gerfin, V. Gramlich, Inorg. Chim. Acta 235 (1995) 215.
[32] V.G. Fritz, G. Becker, D. Kummer, Z. Anorg. Allg. Chem. 372 (1970) 171.
[33] H.H. Karsch, K. Zellner, S. Gamper, G. Muller, J. Organomet. Chem. 414 (1991) C39.
[34] H.H. Karsch, G. Grauvogl, P. Mikulcik, P. Bissinger, G. Muller, J. Organomet. Chem. 465 (1994) 65.
[35] H.H. Karsch, B. Deubelly, J. Riede, G. Muller, J. Organomet. Chem. 342 (1988) C29.
[36] P.B. Hitchcock, M.F. Lappert, P.P. Power, S.J. Smith, J. Chem. Soc. Chem. Commun. (1984) 1669.
[37] D.E. Gindelberger, J. Arnold, Inorg. Chem. 33 (1994) 6293.
[38] Y. You, S.R. Wilson, G. Girolami, Organometallics 13 (1994) 4655.
[39] T.G. Gardner, G.S. Girolami, Organometallics 6 (1987) 2551.
[40] T.G. Gardner, G.S. Girolami, Angew. Chem. Int. Ed. Engl. 27 (1988) 1693.
[41] N.E. Schore, J. Am. Chem. Soc. 101 (1979) 7410.

[42] R.D. Tueting, R.S. Iyer, E.N. Schore, J. Organomet. Chem. 320 (1987) 349 362.
[43] J.R. Bailey, H. Shechter, J. Am. Chem. Soc. 96 (1974) 8115.
[44] P.J. Daff, P. Legzdins, S.J. Rettig, J. Am. Chem. Soc. 120 (1998) 2688.
[45] T.W. Hayton, P.J. Daff, P. Legzdins, S.J. Rettig, B.O. Patrick, Inorg. Chem. 41 (2002) 4114.
[46] M.L.H. Green, D. O'Hare, J.G. Watkin, J. Chem. Soc. Chem. Commun. (1989) 698.
[47] M.L.H. Green, D. O'Hare, P. Mountford, J.G. Watkin, J. Chem. Soc. Dalton Trans. (1991) 1705.
[48] H. Handwerker, M. Paul, J. Blumel, C. Zybill, Angew. Chem. Int. Ed. Engl. 32 (1993) 1313.
[49] T.G. Gardner, G.S. Girolami, J. Chem. Soc. Chem. Commun. (1987) 1758.
[50] E.C. Alyea, R.P. Shakya, A.E. Vougioukas, Transition Met. Chem. 10 (1985) 435.
[51] V. Sum, T.P. Kee, M. Thornton-Pett, J. Organomet. Chem. 438 (1992) 89.
[52] G.M. Gray, C.S. Kraihanzel, J. Organomet. Chem. 241 (1983) 201.
[53] G.M. Gray, K.A. Redmill, Inorg. Chem. 24 (1985) 1279.
[54] G.M. Gray, K.A. Redmill, J. Organomet. Chem. 280 (1985) 105.
[55] G.M. Gray, F.P. Fish, D.K. Srivastava, A. Varshney, M.J. van der Woerd, S.E. Ealick, J. Organomet. Chem. 385 (1990) 49.
[56] G.M. Gray, C.S. Kraihanzel, J. Organomet. Chem. 146 (1978) 23.
[57] H. Schumann, H. Benda, Angew. Chem. Int. Ed. Engl. 9 (1970) 76.
[58] M.L.H. Green, A.K. Hughes, P. Lincoln, J.J. Martin-Polo, P. Mountford, A. Sella, L.L. Wong, J.A. Bandy, T.W. Banks, K. Prout, D.J. Watkin, J. Chem. Soc. Dalton Trans. (1992) 2063.
[59] J.M. Ressner, C.P. Wernett, C.S. Kraihanzel, A.L. Rheingold, Organometallics 7 (1988) 1661.
[60] J.M. Boncella, M.L.H. Green, J. Organomet. Chem. 325 (1987) 217.
[61] J.M. Boncella, M.L.H. Green, D. O'Hare, J. Chem. Soc. Chem. Commun. (1986) 618.
[62] C. Bianchini, D. Dapporto, C. Mealli, A. Meli, Inorg. Chem. 21 (1982) 612.
[63] L. Howarth, L.-L. Wong, J. Chem. Soc. Dalton Trans. (1989) 1385.
[64] S.R. Iyer, D.R. Tueting, N.E. Schore, J. Organomet. Chem. 320 (1987) 339.
[65] N.E. Schore, L.S. Benner, B.E. Labelle, Inorg. Chem. 20 (1981) 3200.
[66] L. Dahlenburg, S. Kerstan, D. Werner, J. Organomet. Chem. 41 (1991) 457.
[67] M. McNeill, R.A. Andersen, R.G. Bergman, J. Am. Chem. Soc. 117 (1995) 3625.
[68] R.A. Andersen, R.A. Jones, G. Wilkinson, J. Chem. Soc. Dalton Trans. (1978) 446.
[69] K. McNeill, R.A. Andersen, R.G. Bergman, J. Am. Chem. Soc. 119 (1997) 11244.
[70] A.W. Holland, R.G. Bergman, Organometallics 21 (2002) 2149.
[71] G.W. Bushnell, M.A. Casado, S.R. Stobart, Organometallics 20 (2001) 601.
[72] R.D. Holmes-Smith, R.R. Stobart, R. Vefghi, M.J. Zaworotko, T.S. Cameron, J. Chem. Soc. Dalton Trans. (1987) 969.
[73] X. Zhou, S. Stobart, Organometallics 20 (2001) 1898.
[74] S.R. Stobart, X. Zhou, R. Cea-Olivares, A. Toscano, Organometallics 20 (2001) 4766.
[75] D.R. Brost, C.G. Burce, L.F. Joslin, R.S. Stobart, Organometallics 16 (1997) 5669.
[76] J.J. De Boer, J.A. Van Doorn, C. Masters, J. Chem. Soc. Chem. Commun. (1978) 1005.
[77] J.P. Genet, C. Pinel, V.R. Vidal, S. Mallart, X. Pfister, M.C. Cano De Andrade, J.A. Laffitte, Tetrahedron Asymmetry 5 (1994) 665.
[78] P.R. Meehan, E.C. Alyea, R.P. Shakya, G. Ferguson, Polyhedron 17 (1998) 11.
[79] D.F. Foster, B.S. Nicholls, A.K. Smith, J. Organomet. Chem. 244 (1983) 159.
[80] P.E. Garrou, Chem. Rev. 81 (1981) 229.
[81] F.L. Joslin, S.R. Stobart, J. Chem. Soc. Chem. Commun. (1989) 504.
[82] D.E. Hendriksen, A.A. Oswald, G.B. Ansell, S. Leta, R.V. Kastrup, Organometallics 8 (1989) 1153.
[83] A.G. Abatjoglou, D.R. Bryant, Organometallics 3 (1984) 932.
[84] E.C. Alyea, G. Ferguson, B.L. Ruhl, R. Shakya, Polyhedron 6 (1987) 1223.
[85] K.J. Hogg, L.S. James, A.G. Orpen, G.P. Pringle, J. Organomet. Chem. 480 (1994) C1.
[86] K.R. Dixon, A.D. Rattray, Inorg. Chem. 16 (1977) 209.
[87] W. Keim, H. Mass, J. Organomet. Chem. 514 (1996) 271.
[88] E.C. Alyea, P.R. Meehan, G. Ferguson, S. Kannan, Polyhedron 16 (1997) 3479.
[89] P.R. Meehan, G. Ferguson, R.P. Shakya, E.C. Alyea, J. Chem. Soc. Dalton Trans. (1997) 3487.
[90] E.C. Alyea, G. Ferguson, R.P. Shakya, P.R. Meehan, Inorg. Chem. 36 (1997) 4749.
[91] M.D. Fryzuk, C.D. Montgomery, Coord. Chem. Rev. 95 (1989) 1.
[92] M.D. Fryzuk, G.R. Giesbrecht, S.J. Rettig, Organometallics 15 (1996) 3329.
[93] M.D. Fryzuk, D.B. Laznoff, R.C. Thompson, S.J. Rettig, J. Am. Chem. Soc. 120 (1998) 10126.
[94] D. Gudat, L.M. Daniels, G.J. Verkade, Organometallics 9 (1990) 1464.
[95] D.Y. Zhou, M. Minato, T. Ito, M. Yamasaki, Chem. Lett. (1997) 1017.
[96] M. Minato, D.Y. Zhou, K.I. Sumiura, R. Hirabayashi, Y. Yamaguchi, T. Ito, J. Chem. Soc. Chem. Commun. (2001) 2654.
[97] D.Y. Zhou, L.B. Zhang, M. Minato, T. Ito, K. Osakada, Chem. Lett. (1998) 187.
[98] T. Ito, K. Shimada, T. Ono, M. Minato, Y. Yamaguchi, J. Organomet. Chem. 611 (2000) 308.
[99] S. Juge, M. Stephan, J.A. Laffitte, J.P. Genet, Tetrahedron Lett. 31 (1990) 6357.
[100] T. Imamoto, T. Oshiki, T. Onozawa, T. Kusumoto, K. Sato, J. Am. Chem. Soc. 112 (1990) 5244.
[101] R.L. Pruett, Adv. Organomet. Chem. 17 (1979) 1.
[102] M.O. Farrell, C.H. Van Dyke, L.J. Boucher, S.J. Metlin, J. Organomet. Chem. 169 (1979) 199.
[103] M. Kranenburg, P.C.J. Kamer, P.W.N.M. van Leeuwen, D. Vogt, W. Keim, J. Chem. Soc. Chem.Commun. (1995) 2177.
[104] L.A. van der Veen, P.H. Keeven, G.C. Schoemaker, J.N.H. Reek, P.C.J. Kamer, P.W.N.M. van Leeuwen, M. Lutz, A.L. Spek, Organometallics 19 (2000) 872.